

1           **Transverse energy analysis of**  
2           **relativistic heavy ion collisions**  
3   **through the use of identified particles**  
4           **spectra**

5                   A Thesis Presented for the  
6                   Master of Science  
7                   Degree  
8           The University of Tennessee, Knoxville

9                   Biswas Sharma

10                  May 2018

11

© by Biswas Sharma, 2018

12

All Rights Reserved.

# 13 Table of Contents

14	<b>1 Introduction</b>	<b>1</b>
15	1.1 A Brief History of the Universe . . . . .	1
16	1.2 Production of Historical Matter . . . . .	1
17	1.3 Motivation of This Thesis . . . . .	2
18	1.4 Organization of The Thesis . . . . .	2
19	<b>2 Theoretical Background</b>	<b>3</b>
20	2.1 Quantum Chromodynamics . . . . .	3
21	2.2 Phase Transitions . . . . .	4
22	2.3 Quark-Gluon Plasma . . . . .	5
23	<b>3 Relativistic Heavy Ion Collisions</b>	<b>7</b>
24	3.1 RHIC and LHC . . . . .	7
25	3.2 Collision Energy and Geometry . . . . .	9
26	3.3 Kinematic Variables . . . . .	11
27	3.4 QGP Evolution . . . . .	13
28	3.5 Detection of Collision Products . . . . .	13
29	3.6 Detection of QGP Signatures . . . . .	15
30	3.6.1 Bjorken Energy Density . . . . .	15
31	3.6.2 Elliptic Flow . . . . .	16
32	3.6.3 Dilepton Production . . . . .	16
33	3.6.4 Direct photons . . . . .	17
34	3.6.5 Strangeness Enhancement . . . . .	18

35	3.6.6 Jet Quenching . . . . .	19
36	<b>4 Measurement of Transverse Energy</b>	<b>22</b>
37	4.1 Definition of Transverse Energy . . . . .	22
38	4.2 $E_T$ Measurement with Calorimeters . . . . .	23
39	4.3 $E_T$ Measurement with Tracking Detectors . . . . .	23
40	4.3.1 Calculation of $\frac{dE_T}{d\eta}$ from $p_T$ spectra . . . . .	24
41	4.3.2 Tracking Detectors in STAR . . . . .	26
42	4.4 The Beam Energy Scan Program . . . . .	26
43	4.4.1 BES Calorimetry . . . . .	28
44	4.4.2 BES $p_T$ spectra . . . . .	28
45	<b>5 Data Analysis</b>	<b>30</b>
46	5.1 Extrapolation of Spectra . . . . .	30
47	5.1.1 Boltzmann-Gibbs Blast Wave . . . . .	30
48	<b>6 Results</b>	<b>31</b>
49	<b>Bibliography</b>	<b>32</b>
50	<b>Appendices</b>	<b>65</b>

# <sup>51</sup> List of Tables

<sup>52</sup>	3.1 Colliding species and associated collision energies at RHIC [24] . . . . .	10
---------------	--	----

# List of Figures

53			
54	2.1	Schematic of the QCD phase diagram [8]. . . . .	6
55	3.1	Initial layout of the RHIC.[26]. . . . .	8
56	3.2	An illustration of a mid-central collision of two nuclei traveling in the z	
57		direction. The X-axis is parallel to the line joining the centers of the two	
58		nuclei at the time of collision. [13]. . . . .	11
59	3.3	An illustration of a collision consisting of participants (solid red) and	
60		spectators (open blue) within the colliding nuclei labeled A and B. $t_c$ denotes	
61		the time of maximum overlap of the two nuclei. The apparent narrowing of	
62		the volumes of the nuclei in the z-direction is due to Lorentz contraction. [37]	12
63	3.4	Evolution of the QGP represented in a lightcone diagram. $\tau_0$ denotes the	
64		formation time of the QGP. $T_c$ is the critical temperature of the transition	
65		from the QGP to the hadron gas phase. $T_{ch}$ and $T_{fo}$ stand for the temperatures	
66		at, respectively, chemical freeze-out and thermal freeze-out. [13] . . . . .	14
67	3.5	Minimum-bias Au+Au ( $\sqrt{s_{NN}} = 200\text{GeV}$ ) elliptic flow spectra for identified	
68		particles: (a) $v_2$ vs $p_T$ and (b) $v_2$ vs $KE_T$ . [4] . . . . .	17
69	3.6	Minimum-bias Au+Au ( $\sqrt{s_{NN}} = 200\text{GeV}$ ) elliptic flow spectra for identified	
70		particles: (a) $\frac{v_2}{n_q}$ vs $\frac{p_T}{n_q}$ and (b) $\frac{v_2}{n_q}$ vs $\frac{KE_T}{n_q}$ . [4] . . . . .	18
71	3.7	Feynman diagram representing the production of a lepton pair from a quark	
72		and an antiquark. [39] . . . . .	19
73	3.8	Feynman diagram representing the production of photons from quarks and	
74		gluons. (a) and (b) represent annihilation processes, whereas (c) and (d)	
75		represent Compton processes.[39] . . . . .	20

76	3.9	Illustration of jet quenching. Two jets are produced from each of the hard	
77		scatterings occuring at the locations of the solid dots. Jets originating closer	
78		to the initial surface are more probable to propagate outside the medium, as	
79		shown. Jets opposite to them interact with the medium, losing their energy	
80		and resulting in bow front shock waves.[36] . . . . .	21
81	4.1	Energy loss distribution in the STAR TPC for primary and secondary	
82		particles. [18]. . . . .	27
83	4.2	Transverse momentum spectra for $\pi^+$ , $\pi^-$ , $K^+$ , $K^-$ , $p$ , and $\bar{p}$ at midrapidity	
84		( $ y  < 0.1$ ) from 39 GeV Au+Au collisions at RHIC. The fitting curves	
85		on the 0-5% central collision spectra for pions, kaons, and protons/anti-	
86		protons represent, respectively, the Bose-Einstein, $m_T$ -exponential, and	
87		double-exponential functions. [2]. . . . .	29

# Chapter 1

## Introduction

### 1.1 A Brief History of the Universe

Nobody knows what happened at the beginning of the Universe. The Big Bang model stands on the pillars of observational evidences, such as the cosmic microwave background radiation and the cosmological expansion, and suggests that at the beginning the universe must have been at a state of really high density and temperature. As the universe expanded, it went through several stages of cooling characterized by the formation of matters with different compositions. The matter we mostly observe today exists at temperatures and densities much lower compared to those in the early universe.

### 1.2 Production of Historical Matter

The Large Hadron Collider (LHC) at CERN and the Relativistic Heavy Ion Collider (RHIC) at the Brookhaven National Laboratory have the ability to collide heavy nuclei, such as those of gold and uranium, at nearly the speed of light, reaching temperatures of trillions of degrees Celcius. These laboratories have provided evidence of the formation of an exotic state of matter, called the quark-gluon plasma (QGP). It only exists for a brief amount of time after such collisions and instantly freezes out into a plethora of new particles, which carry the signatures we can use to deduct QGP properties. Its properties suggest that it should be similar to the matter that existed within microseconds of the genesis of the universe.



107 It reportedly behaves like an almost perfect quantum fluid with no resistance and exhibits  
108 other interesting properties.

### 109 **1.3 Motivation of This Thesis**

110 One of the methods to probe the properties of this matter is by analyzing the conversion of the  
111 beam-direction energy at the time of collision into transverse energy after the collision. This  
112 analysis is generally done by using data from the calorimeters placed around the collision site.  
113 In this thesis, I use the data collected by the tracking detectors, instead of the conventional  
114 calorimeters, to perform the transverse energy analysis.

### 115 **1.4 Organization of The Thesis**

116 This thesis is structured as follows. Chapter 2 touches on the theoretial background  
117 associated with the concept of the quark-gluon plasma. In Chapter 3, I attempt to  
118 summarize the experimental concepts pertaining to heavy-ion collisions, and the production  
119 and detection of QGP. Chapter 4 consists of the formalism of the measurement of transverse  
120 energy using calorimeters as well as tracking detectors. It also gives an example of what has  
121 been done using calorimeters. Chapter 4 describes the data used to perform the analysis in  
122 this thesis and notes down the details of the analysis. In Chapter 5, I present the results  
123 and compare them to the ones in literature obtained using a different method. Chapter 6  
124 concludes the thesis by summarizing it and shedding light on some of its implications.

# Chapter 2

## Theoretical Background

### 2.1 Quantum Chromodynamics

The strong force is one of the four fundamental interactions in physics. At large scale, it is responsible for binding the nucleons together to give the nucleus its structure. At the smaller scale, it binds the fundamental units of subnuclear matter, the quarks, together to form the nucleons. The electrodynamic interaction between charged particles such as protons and electrons is described by quantum electrodynamics (QED) as mediated by photons; the strong interaction, albeit more complicated, is explained under the framework of quantum chromodynamics (QCD) as mediated by gluons. [21, 32] The quarks and gluons of QCD are collectively known as partons. The gluons are the gauge bosons of the Yang-Mills theory.

The Yang-Mills theory is a non-Abelian gauge theory. It has a Lagrangian that is described by several parameters, some of which are redundant and need to be gauged. This is done by a mathematical treatment as prescribed under a gauge theory. The gauge theory associated with the Yang-Mills theory is based on the  $SU(N)$  group. It is non-Abelian as represented by the transformations being non-commutative. QCD is a gauge theory that describes the application of the  $SU(3)$  symmetry transformations on the triplet of quarks, namely red, blue, and green, with the nomenclature having no physical dependence on the three primary colors. The Electroweak interaction, on the other hand, can be formalized

under the gauge group  $SU(2) \times U(1)$ . Together, they form the  $SU(3) \times SU(2) \times (U(1))$  gauge theory called the standard model.

One of the aspects in which QCD is different from QED is the confinement of partons. In QED, the fundamental particles are bound together by the Coulomb potential, which diminishes with distance between the charge-carrying particles, as demonstrated by the relation 2.1:

$$V_C \propto \frac{1}{r} \quad (2.1)$$

where  $V_C$  is the Coulomb potential, and  $r$  is the spatial separation between the particles. This means that bound QED particles can be isolated by increasing their spatial separation. The QCD potential, on the other hand, has an extra linear term in it:

$$V_{QCD} = -\frac{4}{3} \frac{\alpha_S}{r} + kr \quad (2.2)$$

where  $\alpha_S$  is the QCD fine-structure constant and  $k$  is the strength of the color interaction (1 GeV/fm). This means that the potential increases linearly with distance at large distances, and so an infinite amount of energy is required to separate quarks. Hence, we never observe isolated quarks and they are said to be confined, not just bound, to form composite structures called hadrons.[29] Composition of a quark and an anti-quark forms a meson and that of three quarks forms a baryon. In addition to having a color charge, a quark also carries a flavor. There are six different quarks based on the flavors they carry: up, down, top, bottom, beauty, and strange.

## 2.2 Phase Transitions

In everyday life, we observe matter existing in four distinct phases: solid, liquid, gas, and plasma. Changes in physical conditions can lead to a transition from one of these phases to another, exemplified by the commonly observed conversion of ice to water. Distinctions among the various phases can be represented in a chart called the phase diagram.

The phase diagram consists of thermodynamic observables such as temperature and density on its axes. Curves in the phase diagram represent boundaries of physical conditions

at which two or more phases of matter can coexist in equilibrium. Crossing a boundary represents an abrupt transition from one phase to another; this abruptness is mathematically characterized by the discontinuity in the change of the derivative of the free energy – a thermodynamic variable – with respect to the physical quantities in the axes. There can also be regions in the diagram representing the ranges of physical conditions in which a smooth phase transition can take place.

One of the main focuses of current experimental and theoretical nuclear physics research is the study of the phase diagram of strongly interacting matter at a range of temperatures and baryon chemical potentials. In experiments involving the collisions of heavy ions at high and low energies, different regions of the phase diagram can be probed by varying the collision energy [3]. For instance, the high-baryon chemical potential regime corresponds to lower beam energies and higher temperatures correspond to higher beam energies. The results of these experiments and model calculations can be used to study the nature of transitions in the QCD phase diagram.

A schematic representing the QCD phase diagram on the temperature ( $T$ ) and quark chemical potential ( $\mu$ ) plane is shown in Figure 2.1 [8]. A second-order transition is predicted at low baryon chemical potentials (close to baryon-antibaryon symmetry) and high temperatures reminiscent of the early universe. Methods to study this region of the phase space will be explored in this thesis. At low temperatures and high chemical potentials, loose predictions have been made regarding the existence of exotic phases of high density matter, and programs, such as the Compressed Baryonic Matter experiment at the Facility for Antiproton and Ion Research in Germany, are being designed to study this region of the phase diagram.

## 2.3 Quark-Gluon Plasma

The confinement of quarks into the hadronic phase of QCD matter, as described in section 2.1, has its limitations. At very high densities, when the wave function of a single hadron encompasses the spatial regions covered by multiple such hadrons, it is impossible to classify which pair or triplet of quarks belongs to which meson or baryon. As long as a particular

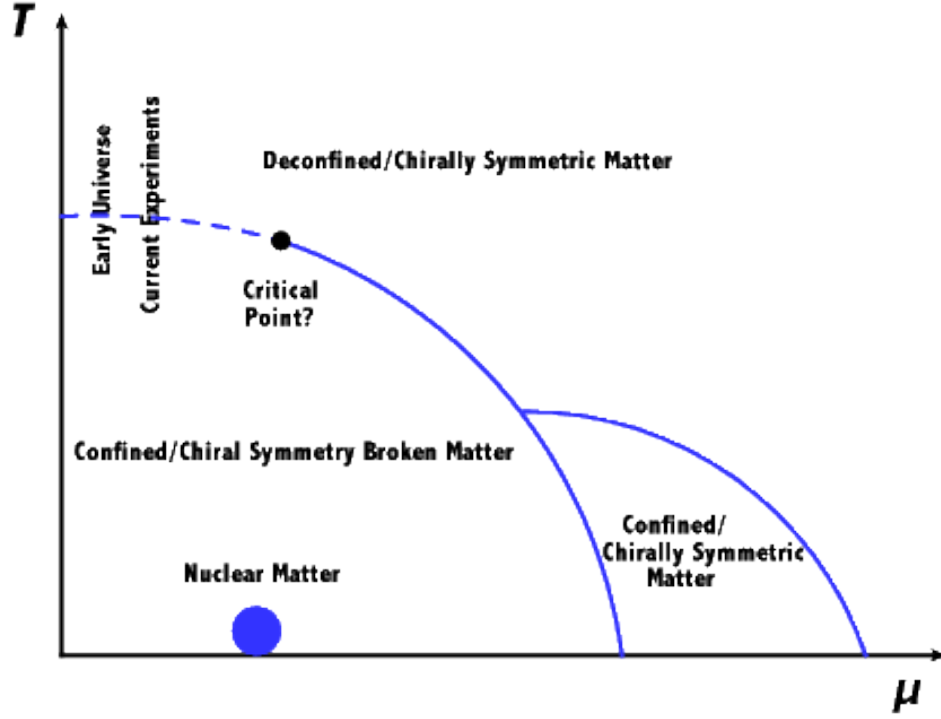


**Figure 2.1:** Schematic of the QCD phase diagram [8].

197 quark is close enough to the other quarks in the volume, it is deconfined in such a way that it  
 198 can freely move anywhere in the volume. [29] QCD predicts such phase transition, at energy  
 199 densities above  $0.2\text{-}1\text{ GeV/fm}^3$  [1] and around a critical temperature of about 200 MeV [23],  
 200 of strongly interacting matter to a phase with quarks and gluons in thermal and chemical  
 201 equilibrium representing the relevant degrees of freedom and behaving like an almost perfect  
 202 quantum fluid [11]. This deconfined state of quarks and gluons is termed the quark-gluon  
 203 plasma (QGP) in analogy to the quantum electrodynamical plasma phase of matter.

## Chapter 3

# Relativistic Heavy Ion Collisions

The experimental evidences of the theoretically appealing existence of QGP come from the collisions of large nuclei. The signatures of such evidence are described in section 3.6. Physicists started noting down such evidences since as far back as 1984, when nuclei were accelerated and collided with stationary targets.[17] They were able to agree on a conclusive discovery of this matter during the 2000s, after colliding accelerated nuclei with other such nuclei or smaller species (protons, deuterons) at unprecedented energies and with improved detection schemes.[34] With further increase in collision energies and enhancement in detector technology, modern accelerator facilities have not only added such evidences but also provided estimates of some of the properties as well as the dynamics of the evolution of the QGP. The following sections describe two such facilities, the physics of the collisions and what happens after the collisions.

### 3.1 RHIC and LHC

The Relativistic Heavy Ion Collider (RHIC) is located in Upton, New York in the premises of the Brookhaven National Laboratory (BNL). Its construction started in 1991 and was completed in 1999. Figure 3.1 shows the layout, at the time of construction, of the collider along with the Alternating Gradient Synchrotron (AGS) complex and the locations of the original four detectors: Solenoidal Tracker At RHIC (STAR), Pioneering High Energy Nuclear Interaction eXperiment (PHENIX), PHOBOS and BRAHMS (Broad RAnge

Hadron Magnetic Spectrometers). PHOBOS and BRAHMS were decommissioned after the completion of their science objectives, but STAR and PHENIX are still functional. The AGS was part of BNL before the construction of the RHIC, and its capabilities were augmented with the construction of the AGS Booster in 1991.

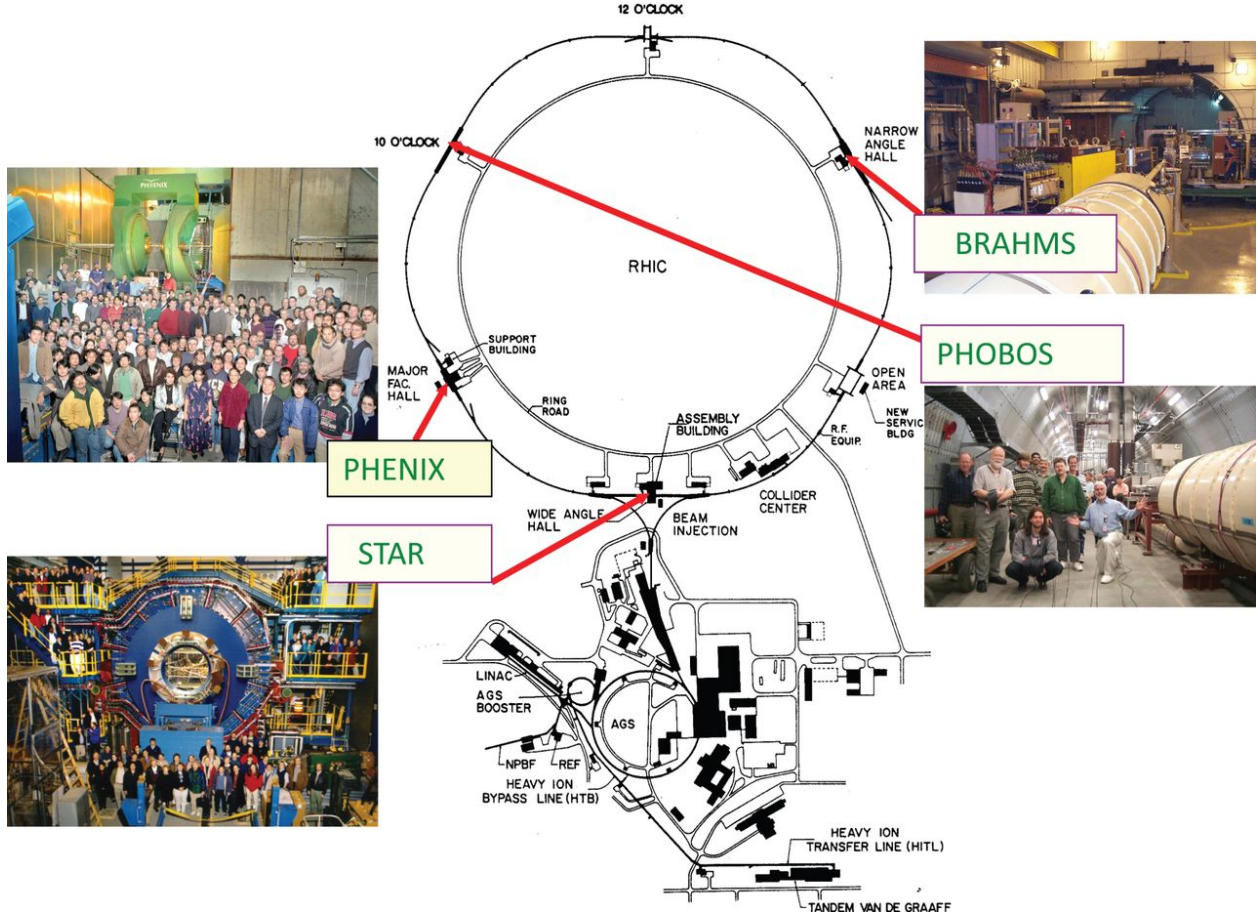


**Figure 3.1:** Initial layout of the RHIC.[26].

227

Heavy ion beams in the RHIC are created in a series of steps before collision. In case of gold ions, a pulsed sputter source produces negatively charged ions, which are stripped of some of their electrons with a foil on the positive end of the high-voltage Tandem Van de Graff. The ions are now positively charged and are accelerated to 1MeV/u toward the negative terminal of the Tandem, upon exiting which some more stripping takes place. The bending magnets then selectively deliver +32 charge states of the ions to the Booster Synchrotron, which accelerates them to 95MeV/u and strips them to +77 charge state before injecting them to the AGS. The AGS accelerates them to 10.8 GeV/u and strips them of

the remaining two electrons at the exit. The gold ions are then injected through the AGS-to-RHIC Beam Transfer Line to the two RHIC rings. These rings carry beams moving in opposite directions and intersect at six symmetric locations in the 3.8 km circumference. The original four detectors are located in four of these six locations where the beams undergo head-on collisions.

The Large Hadron Collider (LHC) is located underground (between 45m and 170m) beneath the France-Switzerland border near the city of Geneva. The two rings of the collider were constructed between 1998 and 2008 by the European Organization for Nuclear Research (CERN) in the 26.7 km circular tunnel originally housing CERN's Large Electron-Positron collider. Analogous to the RHIC, the LHC gets its beams prepared by a series of machines in the CERN accelerator complex. The collisions occur at the locations of the four big LHC experiments: Compact Muon Solenoid (CMS), A Toroidal LHC ApparatuS (ATLAS), Large Hadron Collider beauty (LHCb) experiment, and A Large Ion Collider Experiment (ALICE). ALICE is dedicated to the study of heavy-ion collisions. [15]

## 3.2 Collision Energy and Geometry

What happens in the aftermath of a collision depends on how much energy is available at the time of the collision as well as the geometry of the collision. The experimenter controls the collision energy, so it's known before the collision. The geometry of the collision is deduced from the constraints imposed by the static (eg. rest mass) and dynamic (eg. trajectory) properties of the detected products.

In collision experiments, it is convenient to use a reference frame in which the net momentum of the pair of colliding species is zero. This frame is called the center-of-mass frame. In this frame, the total energy of the species in the two beams is a function of the number of nucleons and the center-of-mass energy per nucleon. In case of symmetric collisions, i.e, collisions involving identical species in the two beams, the collision energy is reported as the center-of-mass energy per nucleon pair,  $\sqrt{s_{NN}}$ . The magnitude of this quantity constrains the species that can be produced from any collision.



263 The RHIC has the unique capability of colliding species at a range of energies spanning  
264 almost two orders of magnitude. Table 3.1 lists the collision energies produced so far at  
265 RHIC for various collision systems. The LHC, on the other hand, boasts the highest amount  
266 of collision energy for any collider on earth. It collided species (p+p, p+A, Pb+Pb) at a  
267 center of mass energy upto 2.76 TeV per nucleon pair at the end of 2010. At the end of  
268 2015, 5.02 TeV Pb-Pb collisions were successfully completed. [16]

Collision system	$\sqrt{s_{NN}}(GeV)$
p+p	200, 500
d+Au	200
Cu+Cu	62, 200
Au+Au	9, 20, 62, 130, 200

**Table 3.1:** Colliding species and associated collision energies at RHIC [24]

269 In general, any collision between two nuclei is not perfectly head-on. Some collisions are  
270 close to being head-on and are called central collisions. Some are far from being head-on and  
271 are called peripheral collisions. The amount by which a collision is central is quantitatively  
272 represented by a variable called centrality. By convention, 0% is the centrality of a perfectly  
273 head-on collision and 100% is that of the least head-on, i.e., the most peripheral collision. In  
274 practice, each collision event is deducted to belong to a specific centrality bin, for instance,  
275 0-5%. Figure 3.2 illustrates the aftermath of a mid-central collision, i.e, a collision in which  
276 about half of the volume of each of the nuclei intersects the other.

277 The collision of two nuclei can be modeled as a set of collisions of the constituents  
278 that make up the nuclei. The constituents that take part in the collisions and are called  
279 participants. The rest of the constituents are known as spectators. Figure 3.3 illustrates the  
280 distribution of participants and spectators in two colliding nuclei. Expectedly, the number  
281 of participants is more in more central collisions.

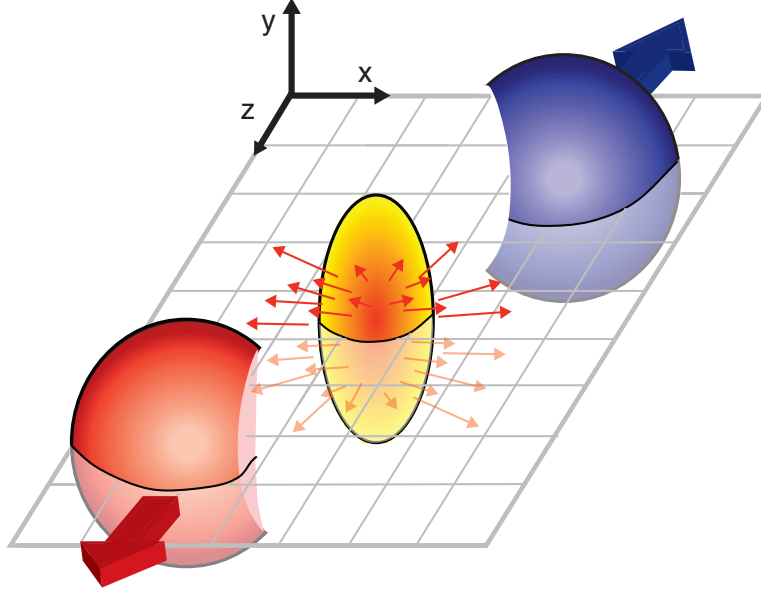


**Figure 3.2:** An illustration of a mid-central collision of two nuclei traveling in the  $z$  direction. The  $X$ -axis is parallel to the line joining the centers of the two nuclei at the time of collision. [13].

### 3.3 Kinematic Variables

The description of the collision physics and the interpretation of its results are aided by the construction of variables that undergo simple transformations under a change of reference frame. Two such variables, rapidity and pseudorapidity, are described in this section.

The rapidity,  $y$ , of a particle is defined as:

$$y \equiv \frac{1}{2} \ln \frac{p_0 + p_z}{p_0 - p_z} \quad (3.1)$$

$$= \frac{1}{2} \ln \frac{E + p_z}{E - p_z}, \quad (3.2)$$

where  $p_0$  and  $p_z$  are the components of its contravariant four-momentum  $p = (p_0, p_x, p_y, p_z)$  with  $p_0 = \frac{E}{c}$ ,  $E$  being the relativistic energy of the particle and  $c$ , the speed of light, being equal to 1 in natural units.

The rapidity of a particle is used as a relativistic description of its velocity. Unlike the canonical velocity of a particle, its rapidity transforms simply additively under a Lorentz

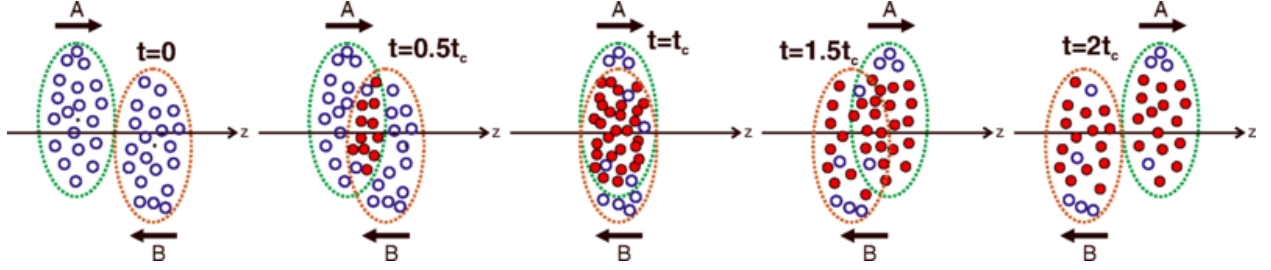


**Figure 3.3:** An illustration of a collision consisting of participants (solid red) and spectators (open blue) within the colliding nuclei labeled A and B.  $t_c$  denotes the time of maximum overlap of the two nuclei. The apparent narrowing of the volumes of the nuclei in the  $z$ -direction is due to Lorentz contraction. [37]

292 boost of the frame of reference. For example, suppose a particle has a rapidity  $y$  in  
 293 a laboratory frame. Let  $y'$  denote its rapidity as measured in a frame that is Lorentz  
 294 boosted with a velocity  $\beta$  in the  $z$ -direction with respect to the laboratory frame. Then the  
 295 relationship between the rapidities in the two different frames is simply

$$y' = y - y_\beta \quad (3.3)$$

296 Here,

$$y_\beta = \frac{1}{2} \ln \frac{1 + \beta}{1 - \beta} \quad (3.4)$$

297 is the rapidity the particle would have in the laboratory frame if it were moving with a  
 298 velocity  $\beta$  in the  $z$ -direction with respect to the laboratory frame, as can be verified from  
 299 equation 3.1 with  $p_0 = \gamma m$  and  $p_z = \gamma \beta m$ ,  $\gamma$  being the Lorentz factor  $\frac{1}{\sqrt{1-\beta^2}}$ . [39]

300 The convenience provided by this construct comes with a cost. As evident from equation  
 301 3.1, the calculation of the rapidity of a particle requires the measurement of two different  
 302 observables associated with it, such as the energy and the  $z$ -direction momentum. However,  
 303 experimental constraints may sometimes only facilitate the measurement of the direction of  
 304 the detected particle with respect to the beam axis. What's more convenient in such a case  
 305 is the use of another variable construct called pseudorapidity,  $\eta$ , defined as:

$$\eta \equiv -\ln \tan \frac{\theta}{2}, \quad (3.5)$$

where  $\theta$  is the angle the particle's momentum vector,  $\mathbf{p}$ , makes with the  $z$ -direction. The above equation can also be written in terms of the momentum as:

$$\eta = \frac{1}{2} \ln \frac{|\mathbf{p}| + p_z}{|\mathbf{p}| - p_z} \quad (3.6)$$

From equations 3.1 and 3.6, it is evident that  $\eta \approx y$  when  $|\mathbf{p}| \approx p_0$ , i.e., when the momentum is large. The transformation of the particle distribution from the  $y$ -space to the  $\eta$ -space is discussed in section 4.3.1.

### 3.4 QGP Evolution

The evolution of the QGP is shown in a lightcone diagram in figure 3.4. The initial state of the colliding nuclei is not well known and is the topic of research for upcoming experiments. During the collision, the participants scatter off of each other while the spectators don't and keep traveling almost unperturbed in their original direction. The immediate aftermath of a central collision of heavy ions at RHIC and LHC energies is the formation of a hot fireball. This fireball evolves in time to form a liquid-like medium of quarks and gluons. This medium attains a local equilibrium and remains in such a state, depending on the collision energy, for about 1-10 fm/c. This equilibrium is broken as the liquid QGP evolves by expanding and cooling to attain a density and temperature at which the deconfinement of quarks and gluons is lost and they undergo a chemical freeze-out to form a hadron gas. Collisions between the constituents of this gas become scant as it evolves with further expansion and cooling, and the hadrons undergo a thermal freeze-out to attain their final energies and momenta.

### 3.5 Detection of Collision Products

Detectors are placed around the collision site to perform measurements on the final state particles emitting from the thermal freeze-out of the medium. These measurements typically include the estimation of the location and time of production of the final states, the type of particle, and the momentum and energy it carries.

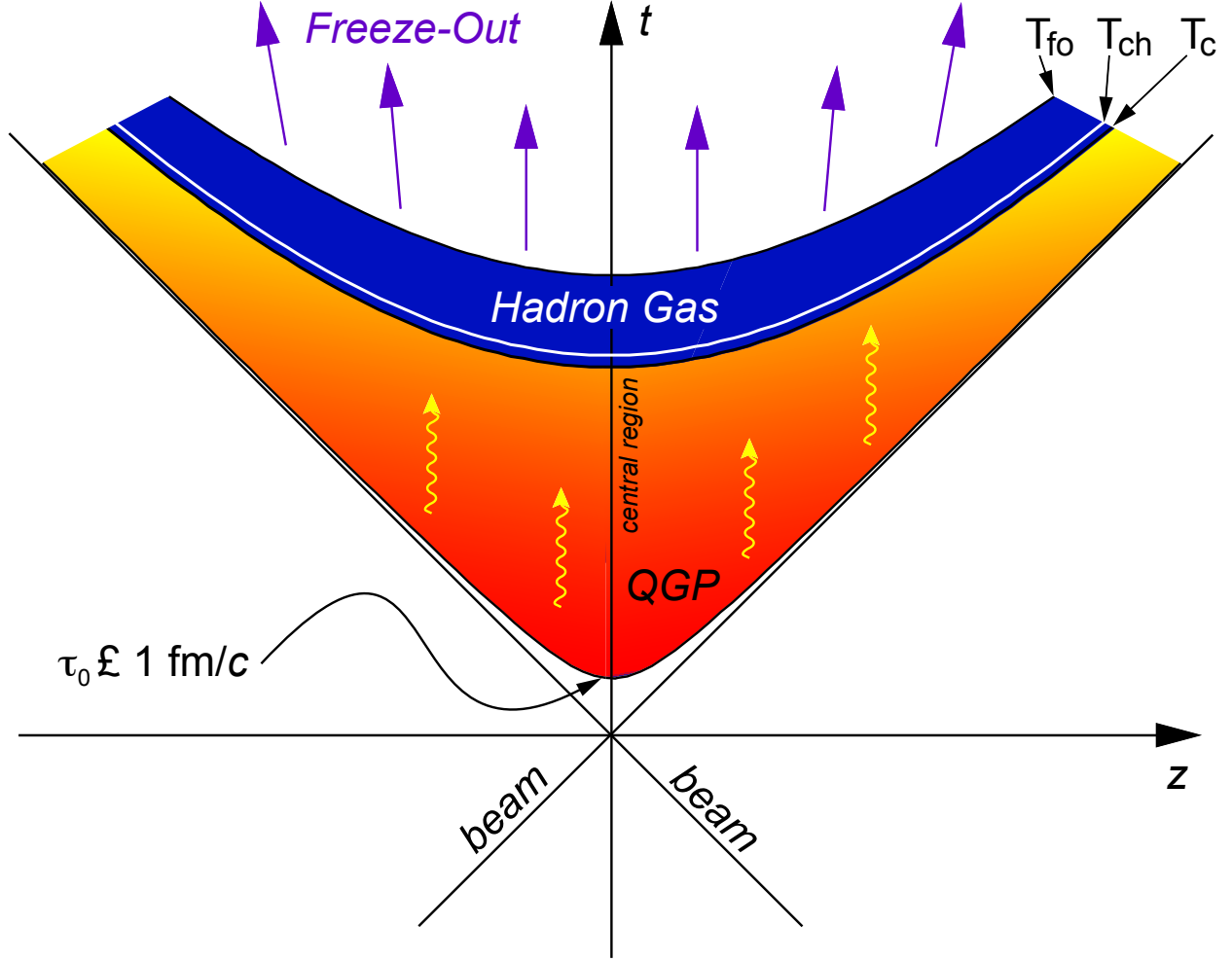


**Figure 3.4:** Evolution of the QGP represented in a lightcone diagram.  $\tau_0$  denotes the formation time of the QGP.  $T_c$  is the critical temperature of the transition from the QGP to the hadron gas phase.  $T_{ch}$  and  $T_{fo}$  stand for the temperatures at, respectively, chemical freeze-out and thermal freeze-out. [13]

329 Generally, a tracking detector surrounds the collision site, and there are calorimeters  
 330 followed by particle identifiers around it. A magnetic field is applied parallel to the beam  
 331 direction around the collision site. Due to this orientation of the magnetic field, the spectators  
 332 traveling parallel to it move undeflected and the final state charged particles with components  
 333 of velocity transverse to the beam axis get deflected around the beam axis with angular  
 334 frequency given by

$$\omega = \frac{qB}{m}, \quad (3.7)$$

where  $q$  is the electric charge of the particle,  $m$  is its mass and  $B$  is the applied magnetic field. Two kinds of detectors most relevant to this thesis, tracking detectors and calorimeters, are described in chapter 4.

## 3.6 Detection of QGP Signatures

The existence and properties of the QGP in the aftermath of high-energy heavy-ion collisions can be probed using different techniques relevant to several theoretical characteristics of the phase. No such signature can alone be used to claim the production of the QGP, and some of the probes, which should be interpreted together, are described below.

### 3.6.1 Bjorken Energy Density

In 1983, J.D. Bjorken[10] prescribed a formula to use the final state particles to estimate the initial energy density,  $\epsilon_0$ , in a nucleus-nucleus collision. With slight changes in the original formula, the energy density is given by:

$$\epsilon_0 = \frac{1}{\tau_0 A_T} \left\langle \frac{dET}{dy} \right\rangle, \quad (3.8)$$

where  $\tau_0$  is the proper time at the moment of QGP equilibration,  $A_T$  is the transverse area of the intersection of the two nuclei, and  $\langle \frac{dET}{dy} \rangle$  is the mean transverse energy per unit rapidity.  $\tau_0$  is model-dependent and is normally of the order of  $1 fm$ .  $A_T$  depends on the centrality of the collision.  $\langle \frac{dET}{dy} \rangle$  is found from the measurement of the transverse energy carried by the final state particles from the collision and is the central theme of this thesis. Details about it are in the following chapters. The estimate of the initial energy density from Bjorken formula can be compared with the QCD prediction of the critical energy density[1] to check if the results from a collision imply the achievement of the critical physical condition required for the phase transition.[20]

### 3.6.2 Elliptic Flow

For yet unknown reasons, the evolution of the medium produced after relativistic heavy ion collisions can be well described under the framework of relativistic hydrodynamics. [30, 35] This description indicates the presence of a collective flow, and hence a liquid-like and thermalized nature, of the constituents that make up the system. The momentum distribution of the final state particles emitting out of the collectively flowing system can be decomposed into its azimuthal Fourier components. The second harmonic coefficient,  $\nu_2(y, p_T)$ , of this decomposition characterizes what is known as the elliptic flow.[19] The magnitude of the elliptic flow from a non-central collision represents the anisotropy in azimuthal momentum space of the thermalized post-collision system.[33]

The elliptic flow of the medium, as a function of the momentum or the kinetic energy in the transverse direction, points towards quarks, rather than hadrons, being the relevant degrees of freedom in the QGP. Figure 3.5 shows  $\nu_2$  plotted against the transverse momentum and the transverse kinetic energy for identified particles. The spectra scale consistently at lower values of both  $p_T$  and  $KE_T$ . However, they branch out at higher values:  $p_T \gtrsim 2\text{GeV}/c$  and  $KE_T \gtrsim 1\text{GeV}$ . Figure 3.6, on the other hand, is similar to figure 3.5, with the exception that both the axes have quantities that are normalized by the number of quarks,  $n_q$ . In this case, the  $KE_T$  spectra strongly exhibits ( $p_T$  does so less strongly) a scaling which is more comprehensively consistent with the number of quarks than in case of figure 3.5. This universal quark-number scaling can be interpreted as the degrees of freedom of the system being quark-like.[4]

### 3.6.3 Dilepton Production

When the color degree of freedom is liberated in the post-collision system, a quark can interact with an antiquark to produce a virtual photon which decays into a lepton and an antilepton. This pair of leptons is devoid of a color charge and can interact with the particles in the fireball only electromagnetically. This leads to them having a significantly larger mean-free path as compared to colored probes, and the number of collision they undergo before reaching a detector is negligible. However, the thermodynamic state of the fireball

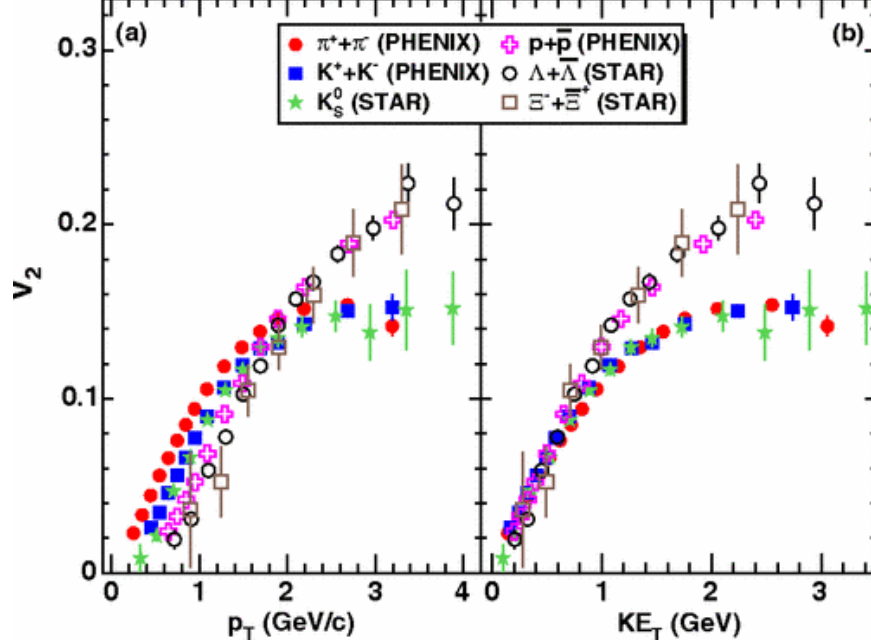


**Figure 3.5:** Minimum-bias Au+Au ( $\sqrt{s_{NN}} = 200 \text{ GeV}$ ) elliptic flow spectra for identified particles: (a)  $v_2$  vs  $p_T$  and (b)  $v_2$  vs  $KE_T$ . [4]

384 affects the momenta of the quarks and the antiquarks, which in turn affect the momenta and  
 385 the production rates of the lepton pairs. Specifically, the temperature of the QGP can be  
 386 estimated using the dilepton spectra. The caveat of doing so is that the QGP is not the only  
 387 possible source of dileptons. Hence, the contributions from other sources, mainly the Drell-  
 388 Yan process, must be figured out before using the dilepton spectra as a QGP diagnostic.  
 389 [39]

### 390 3.6.4 Direct photons

391 In the QGP, a quark and an antiquark can annihilate to produce a photon and a gluon.  
 392 It is also possible for the pair to annihilate and produce two photons, but the probability  
 393 of this process is smaller than the former by about two orders of magnitude. Furthermore,  
 394 a quark (or an antiquark) can interact with a gluon to produce an antiquark (or a quark)  
 395 and a photon, a process analogous to Compton scattering in QED. Just like the leptons  
 396 described in the previous section, the photons produced in the QGP can only interact with  
 397 the medium electromagnetically. Therefore, they undergo minimal scattering before being  
 398 detected, and hence can be used to probe the thermodynamical state of the medium at the



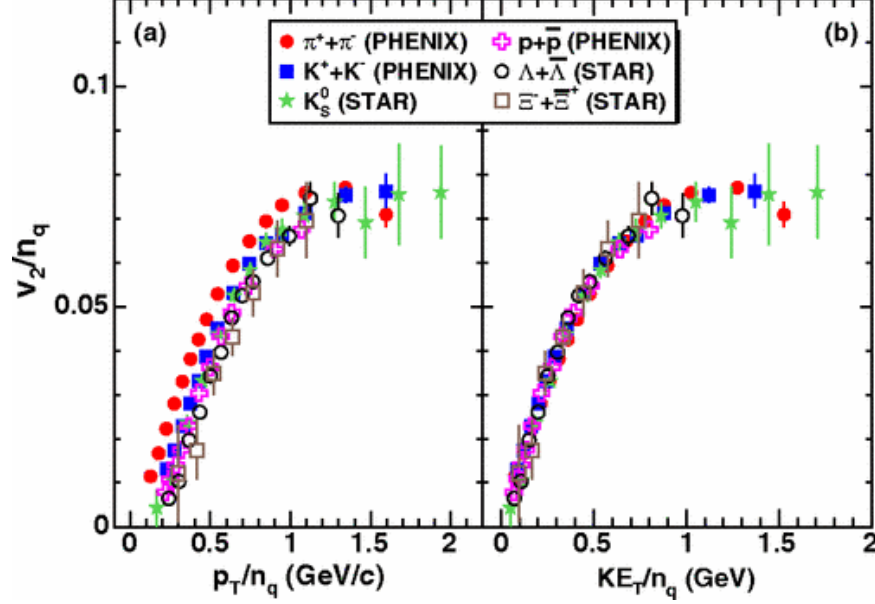


**Figure 3.6:** Minimum-bias Au+Au ( $\sqrt{s_{NN}} = 200\text{GeV}$ ) elliptic flow spectra for identified particles: (a)  $\frac{v_2}{n_q}$  vs  $\frac{p_T}{n_q}$  and (b)  $\frac{v_2}{n_q}$  vs  $\frac{KE_T}{n_q}$ . [4]

time of their creation.[39] Photons can also be produced after hadronization as a result of the scattering of the hadrons within the evolved medium. However, the nature of the  $p_T$  distribution is different in this case, and this difference helps distinguish these photons from the direct photons produced by partonic interactions.[38]

### 3.6.5 Strangeness Enhancement

The interacting nuclei carry no net strangeness before colliding, and so a post-collision observation of strange and multi-strange particles can be a signal for an antecedent existence of deconfined quarks and gluons [14]. Strangeness can also be produced in hadron-hadron collisions. However, it is enhanced in nucleus-nucleus collisions in which a large number of hadrons are produced and are in chemical equilibrium at very high temperatures. Consider the ratio of the production of the strange kaons to that of the non-strange pions, which are the most abundant hadrons produced from nucleus-nucleus collisions. Kaon yield increases more rapidly than does pion yield as the temperature increases. This can be shown mathematically by treating the system as a hadron gas in thermal and chemical equilibrium that follows the Bose-Einstein distribution, but it is beyond the scope of this thesis.[39]

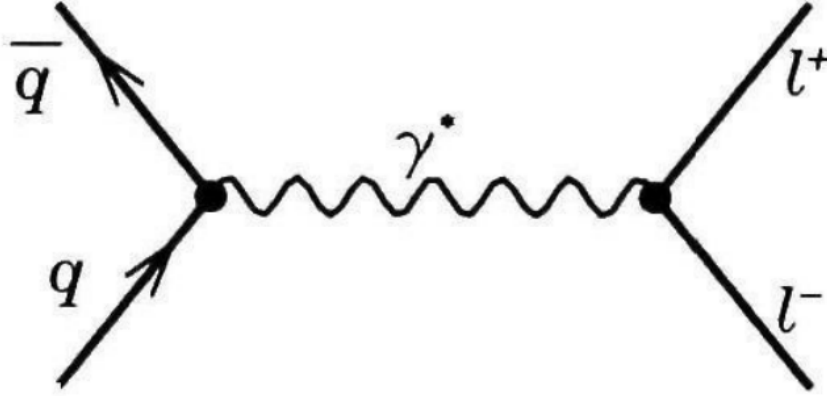


**Figure 3.7:** Feynman diagram representing the production of a lepton pair from a quark and an antiquark. [39]

### 3.6.6 Jet Quenching

A scattering event in which the participants transfer a large amount of their original momenta is called hard scattering. The products of the scattering, carrying high transverse momenta in opposite directions, are called jets. In heavy-ion collisions, most of the hard scatterings are the results of two partons from the opposite nuclei scattering off of each other. These partons can lose their momenta by strongly interacting with a medium made of deconfined quarks and gluons. Therefore, the properties of the jets, as carried by the final state hadrons, should be different for collisions that produce the QGP as compared to those that don't, and hence they can be used as signatures and probes of QGP. Figure 3.9 illustrates the quenching of jets that have to travel long distances in the medium. Formalisms developed to study jet quenching due to radiative and collisional energy losses are detailed in [28].

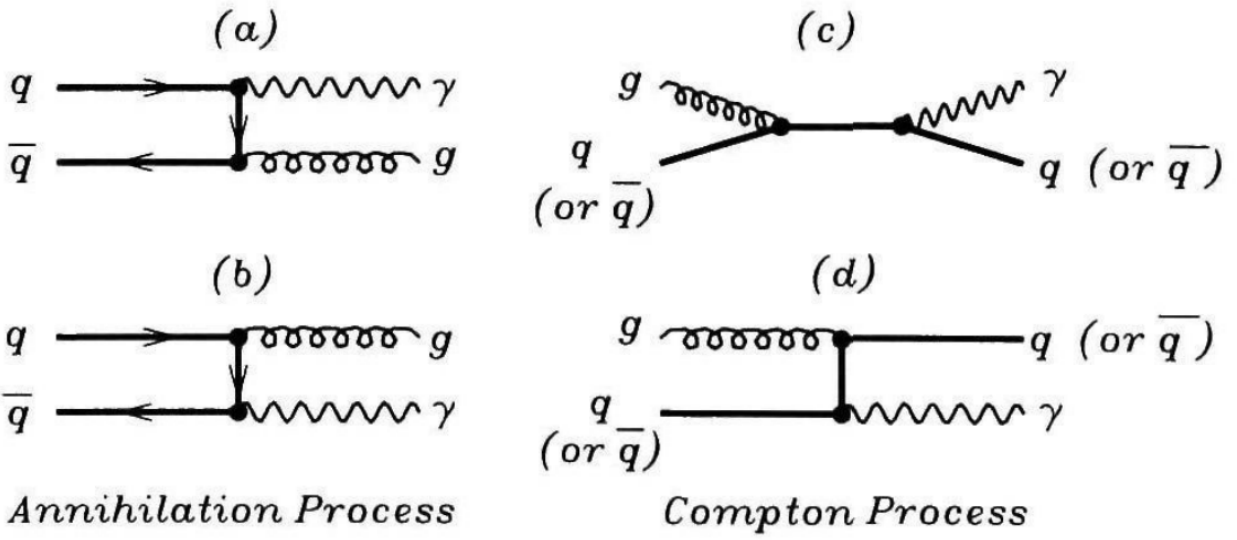


**Figure 3.8:** Feynman diagram representing the production of photons from quarks and gluons. (a) and (b) represent annihilation processes, whereas (c) and (d) represent Compton processes.[39]

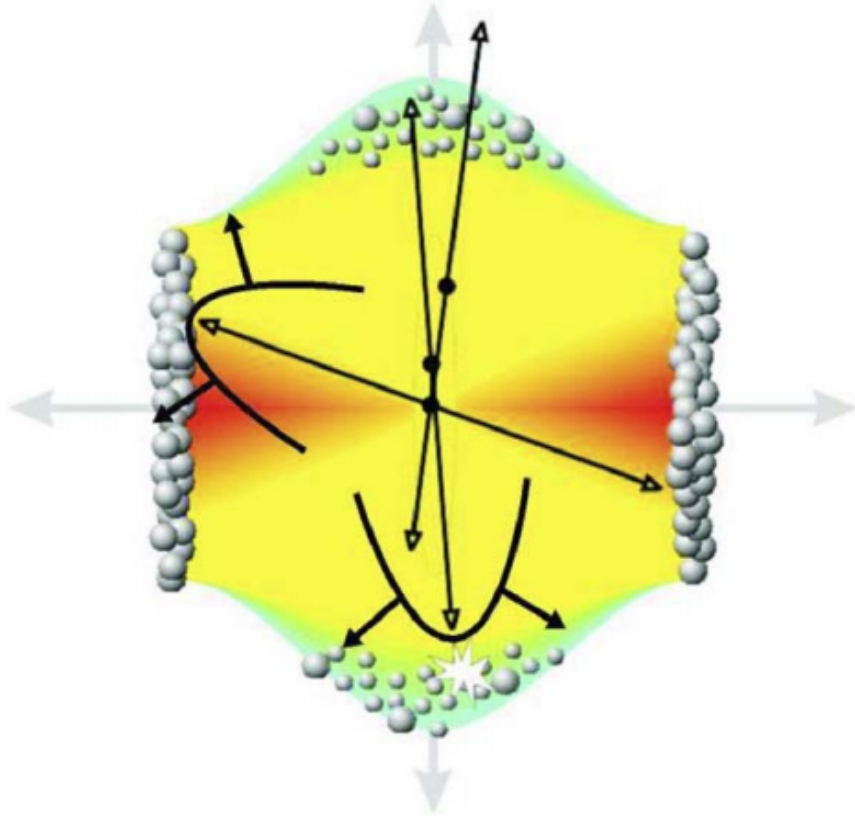


**Figure 3.9:** Illustration of jet quenching. Two jets are produced from each of the hard scatterings occurring at the locations of the solid dots. Jets originating closer to the initial surface are more probable to propagate outside the medium, as shown. Jets opposite to them interact with the medium, losing their energy and resulting in bow front shock waves.[36]

# Chapter 4

## Measurement of Transverse Energy

This chapter introduces the definitions of transverse energy, ways to measure it using different detectors, and particular examples from the STAR detector.

### 4.1 Definition of Transverse Energy

In theory,  $E_T$  from a collision can be defined as the sum of the transverse masses,  $m_T$ , of all the particles produced in the collision, i.e.,

$$E_T \equiv \sum_i m_{T,i} \quad (4.1)$$

with

$$m_T \equiv \sqrt{p_T^2 + m^2} \quad (4.2)$$

where  $m$  is the rest mass of the particle and  $p_T$  is its transverse momentum. Using this definition to calculate the  $E_T$  requires perfect identification of all the particles. It has not been possible to do so in experiments, and so a more feasible, operational definition of  $E_T$  is fabricated. A commonly accepted definition in case of the feasibility of calorimetric measurements is [5, 11]:

$$E_T = \sum_i E_i \sin \theta_i, \quad (4.3)$$

$$\frac{dE_T}{d\eta} = \sin\theta \frac{dE}{d\eta}, \quad (4.4)$$

where the index  $i$  runs over all the particles going into a fixed solid angle for each event,  $\theta$  is the polar angle, i.e, the angle with respect to the beam axis,  $\eta$  is the pseudorapidity defined as

$$\eta \equiv -\ln \tan \frac{\theta}{2}, \quad (4.5)$$

and  $E_i$  is the energy deposited in the calorimeter by the  $i^{th}$  particle.  $E_i$  is considered to be, by convention [6], the following

$$E_i = \begin{cases} E_i^{tot} - m_0 & \text{for baryons} \\ E_i^{tot} + m_0 & \text{for anti-baryons} \\ E_i^{tot} & \text{otherwise} \end{cases} \quad (4.6)$$

where  $E_i^{tot}$  is the total energy of the  $i^{th}$  particle defined canonically as

$$E^{tot} \equiv \sqrt{p^2 + m_0^2} \quad (4.7)$$

and  $m_0$  is the particle's rest mass. In order to account for the portion of the emitted transverse energy not detected or overestimated by the calorimeters, corrections are made based on GEANT simulations.

## 4.2 $E_T$ Measurement with Calorimeters

## 4.3 $E_T$ Measurement with Tracking Detectors

Transverse energy analysis can be done using tracking detectors as well if they are able to produce measurements of other physical quantities that implicitly contain information about the transverse energy. Specifically, the charged particle multiplicity distributions with respect to the transverse momenta can be used to calculate the particle's transverse energy pseudorapidity density. In fact, since the corrections related to the tracking detectors are

very different from those related to the calorimeters, results from the two different methods can be used to test the assumptions involved in each.

The tracking detectors in experiments such as the STAR (Solenoidal Tracker At RHIC) experiment and ALICE (A Large Ion Collider Experiment) at CERN include Time Projection Chambers (TPCs) and Time-of-Flight (TOF) detectors that can give us the  $p_T$  spectra, yields and particle ratios of the identified charged hadrons [27, 2]. The TPCs provide measurements of particle trajectories – that can be used to determine the momenta for low-momentum particles – and of their specific energy loss,

$$\frac{dE}{dx}, \quad (4.8)$$

which can be used with the trajectories to make particle identifications (PID) using the Bethe-Bloch formula [9]. TOF detectors, on the other hand, cover the high-momentum part of the measurements. In ALICE, the combination of the measurements of the TPC with those of the Inner Tracking System (ITS) effectively adds the tracking length, thereby improving the resolution of the measured  $p_T$  spectrum. Details about the PID and momentum determination capabilities of the detectors in ALICE can be found in [12].

The  $p_T$  spectra, available as the counts  $\frac{d^2N}{dydp_T}$  with respect to  $p_T$ , can be used to calculate  $\frac{dE_T}{d\eta}$  as formulated in the following section.

### 4.3.1 Calculation of $\frac{dE_T}{d\eta}$ from $p_T$ spectra

In relativistic heavy ion collisions, rapidity ( $y$ ) is defined as follows:

$$y \equiv \frac{1}{2} \ln \frac{E + p_z}{E - p_z}, \quad (4.9)$$

where  $E$  is given by equation 4.7 and  $p_z$  is the component of the momentum parallel to the beam axis. Pseudorapidity,  $\eta$ , is just  $y$  with  $m_0 = 0$ :

$$\begin{aligned}\eta &= \frac{1}{2} \ln \frac{p + p_z}{p - p_z} \\ &= \frac{1}{2} \ln \frac{1 + \cos \theta}{1 - \cos \theta} \\ &= \frac{1}{2} \ln \frac{2 \cos^2 \frac{\theta}{2}}{2 \sin^2 \frac{\theta}{2}}\end{aligned}$$

$$\therefore \eta = -\ln \left| \tan \frac{\theta}{2} \right| \quad (4.10)$$

473 Note that the absolute value is not necessary for  $0 \leq \theta \leq \pi$ . Then, taking the exponential  
474 of both sides of the above equation and using Euler's formula, we get:

$$\sin \theta = \frac{1}{\cosh \eta}. \quad (4.11)$$

Hence,

$$\begin{aligned}p &= \frac{p_T}{\sin \theta} \\ &= p_T \cosh \eta,\end{aligned}$$

475 and so we have

$$E_T = E \sin \theta = \frac{\sqrt{p_T^2 \cosh^2 \eta + m_0^2}}{\cosh \eta} \quad (4.12)$$

476 The Jacobian for the transformation from  $y$ -space to  $\eta$ -space is derived, by differentiating  
477  $y$  with respect to  $\eta$  (obtained from equations 4.9 and 4.10), to be:

$$\frac{\partial y}{\partial \eta} = \frac{p_T \cosh \eta}{\sqrt{m_0^2 + p_T^2 \cosh^2 \eta}} \quad (4.13)$$



From equations 4.12 and 4.13, we can see that the product of  $E_T$  with the Jacobian is equal to  $p_T$ . That leads to a formulation of  $\frac{dE_T}{d\eta}$  as a function of only  $\eta$  and  $p_T$ :

$$\frac{dE_T}{d\eta} = \frac{1}{2a} \int_0^{10\text{GeV}/c} \int_{-a}^a p_T \frac{d^2 N}{dy dp_T} d\eta dp_T \quad (4.14)$$

where  $a$  and  $-a$  are the bounds for  $\eta$ .

### 4.3.2 Tracking Detectors in STAR

In the STAR experiment, the TPC is the primary tracking detector. It is 4.2 m long and it cylindrically enshrouds the accelerator beam pipe from its outside, with an inner diameter of 1 m and an outer diameter of 4 m [24]. It covers a pseudorapidity range of  $|y| < 1.8$  in all of azimuth in terms of acceptance of charged particles. It can identify particles with momenta over 100 MeV/c up to about 1 GeV/c as well as measure their momenta from 100 MeV/c to 30 GeV/c [7]. Figure 4.1 shows the PID capability of the STAR TPC for very high-multiplicity events [18]. Separation of pions from protons is demonstrated up to a little more than 1 GeV/c. At higher momenta, separating particles is more difficult because their energy loss has lower dependence on the rest mass [7]. The TOF system in STAR, with a time resolution of  $\lesssim 100$  ps, aids PID at higher momenta. However, at intermediate  $p_T$ , between  $\approx 2.0$  and 4.0 GeV/c, the TPC by itself cannot distinguish between pions and protons and the TOF by itself cannot separate pions from kaons. This problem is resolved by utilizing the fact that the dependence of the particle velocity on  $p_T$  – in case of the TPC – is different from that of the energy loss on  $p_T$  in case of the TPC; combining the results from the two, hence, makes PID feasible in this  $p_T$  range. [31]

## 4.4 The Beam Energy Scan Program

The RHIC, in 2010, started a multi-phase Beam Energy Scan (BES) program to study the QCD phase diagram. The collider has the unique facility to collide nuclei at a range of center-of-mass energies per nucleon,  $\sqrt{s_{NN}}$ . It also has two different detectors that are currently operational, STAR and PHENIX (Pioneering High Energy Nuclear Interactions

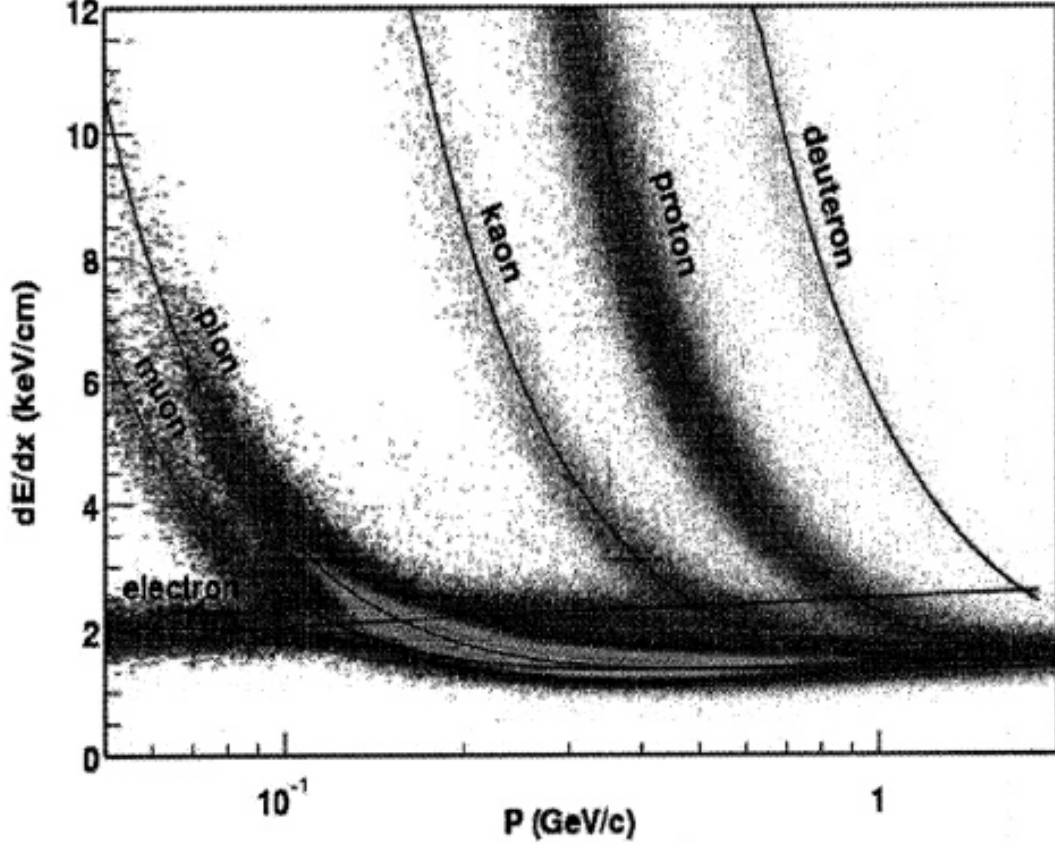


**Figure 4.1:** Energy loss distribution in the STAR TPC for primary and secondary particles. [18].

502 eXperiment), which facilitate the cross-checking of results. Between 2010 and 2011, under  
 503 the exploratory phase I of the BES program, 7.7, 11.5 (not completed in PHENIX), 19.6,  
 504 27, and 39 GeV collisions were completed using pairs of Au nuclei. Together with the  
 505 data formerly collected by the RHIC at higher collision energies, BES phase I data can  
 506 scan the interval from 450 MeV to 20 MeV in  $\mu_B$  space [25, 22]. One of the things that  
 507 can be studied with the data associated with this region of the phase space is statedly the  
 508 possibility of a “turn-off of new phenomena already established at higher RHIC energies”  
 509 (<https://drupal.star.bnl.gov/STAR/starnotes/public/sn0493>). Results corresponding to the  
 510 high- $\mu_B$  region might provide evidence of a first order phase transition, and possibly the  
 511 critical point [22].

512 The manifestation of such phenomena would be in terms of the fluctuations in the  
 513 properties of the post-collision system. One can, for instance, study the scaling of the

transverse energy after the collision with the longitudinal energy at the time of the collision,  
 $\sqrt{s_{NN}}$ . This can be done in multiple ways for a detector like STAR or PHENIX that is made  
up of sub-systems such as the TOF detectors, TPCs/Time Expansion Chambers, as well as  
calorimeters.

#### 4.4.1 BES Calorimetry

Adare et al. [3] use calorimetry in PHENIX to analyze the transverse energy corresponding  
to several different pairs of species colliding at a range of energies. They use the raw  
transverse energy measured by the EMCal,  $E_{EMC}$ , to obtain the total hadronic  $E_T$  by  
making corrections in three different steps. They first scale the data by a constant factor  
calculated to account for the fiducial acceptance in azimuth and pseudorapidity. The second  
factor is calculated to adjust for the effects of the calorimeter towers that are disabled. The  
third factor,  $k$ , is computed as follows

$$k = k_{response} \times k_{inflow} \times k_{losses} \quad (4.15)$$

where  $k_{response}$  corresponds to hadronic particles only depositing a fraction of their total  
energy while passing through the EMCal,  $k_{inflow}$  is attributable to the energy deposited  
by particles coming from outside the EMCal's fiducial aperture, and  $k_{losses}$  accounts for  
the energy not registered in the EMCal due to energy thresholds, edge effects, and more  
importantly due to the particles that make it into the fiducial aperture but decay into  
products outside the aperture.

#### 4.4.2 BES $p_T$ spectra

This thesis details the method of transverse energy analysis through the use of  $p_T$  spectra  
from the STAR BES data. As described in section 4.3.2, the TPCs and TOF detectors in  
STAR can identify particles as well as their trajectories and ultimately their multiplicity  
distributions with respect to the momenta. Adamczyk et al. [2] report the results for the  
 $p_T$  spectra for six different identified hadrons,  $\pi^+$ ,  $\pi^-$ ,  $K^+$ ,  $K^-$ ,  $p$ , and  $\bar{p}$ , from the STAR  
experiment. The spectra come from Au+Au collisions – at  $\sqrt{s_{NN}} = 7.7, 11.5, \text{ and } 39 \text{ GeV}$

in the year 2010 and at  $\sqrt{s_{NN}} = 19.6$  and 27 GeV in 2011 – under the BES Program. Figure 4.2 [2] shows the spectra corresponding to 39 GeV collisions categorized into seven different collision centrality classes. These spectra, and their counterparts for the rest of the energies, were used to calculate an estimate of the total transverse energy per event per particle species. This result was then used to estimate the total transverse energy due to all the collision products.

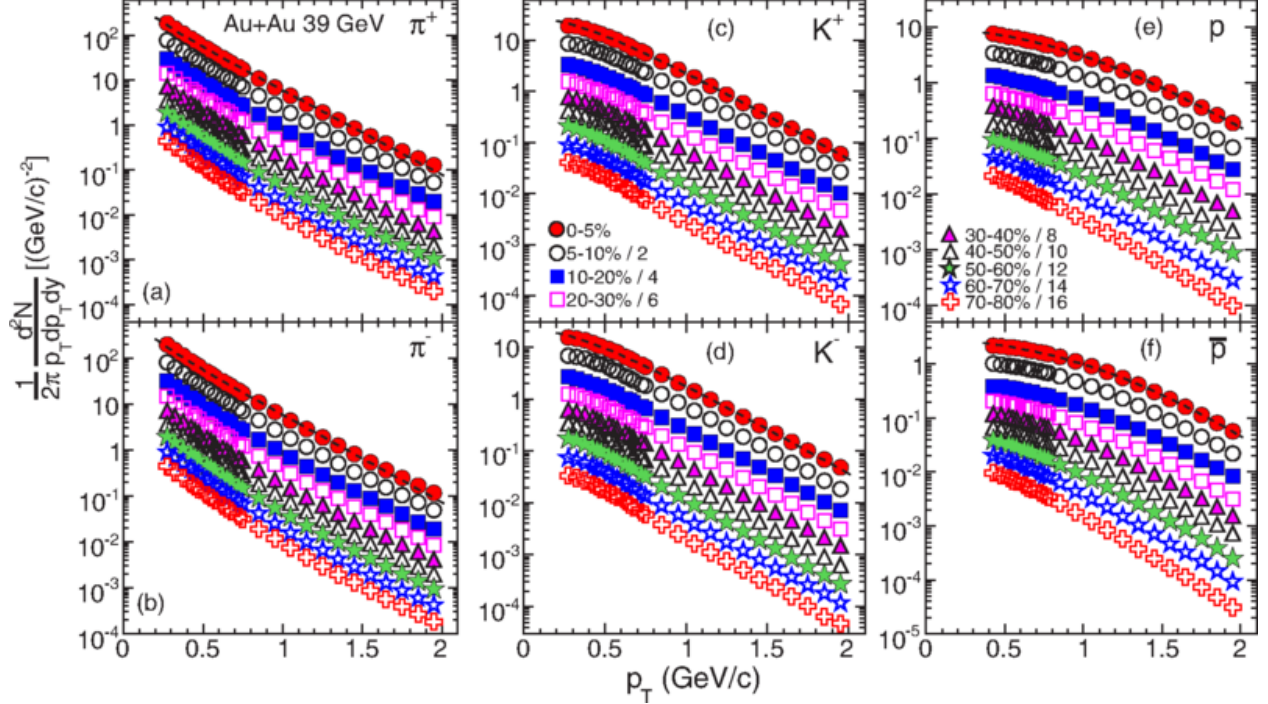


**Figure 4.2:** Transverse momentum spectra for  $\pi^+$ ,  $\pi^-$ ,  $K^+$ ,  $K^-$ ,  $p$ , and  $\bar{p}$  at midrapidity ( $|y| < 0.1$ ) from 39 GeV Au+Au collisions at RHIC. The fitting curves on the 0-5% central collision spectra for pions, kaons, and protons/anti-protons represent, respectively, the Bose-Einstein,  $m_T$ -exponential, and double-exponential functions. [2].

The corrections applied by Adamczyk et al. [2] to the raw data to obtain the spectra and the reported systematic uncertainties in their results are discussed below (under construction)

// Next section will contain the method of extrapolation and the section after that will explain the analysis using the root framework. Then comes the results section, which I will add after I finish analyzing all the data and get all the results including for lambdas.

## 550 Chapter 5

## 551 Data Analysis

### 552 5.1 Extrapolation of Spectra

#### 553 5.1.1 Boltzmann-Gibbs Blast Wave

## 554 Chapter 6

## 555 Results

556 Present results and comparisons to Adare et al.

# Bibliography

558 [1] Adam, J., Adamova, D., Aggarwal, M. M., Aglieri Rinella, G., Agnello, M., Agrawal,  
 559 N., Ahammed, Z., Ahmad, S., Ahn, S. U., Aiola, S., Akindinov, A., Alam, S. N., Silva  
 560 De Albuquerque, D., Aleksandrov, D., Alessandro, B., Alexandre, D., Alfaro Molina,  
 561 J. R., Alici, A., Alkin, A., Millan Almaraz, J. R., Alme, J., Alt, T., Altinpinar, S.,  
 562 Altsybeev, I., Alves Garcia Prado, C., Andrei, C., Andronic, A., Anguelov, V., Anticic,  
 563 T., Antinori, F., Antonioli, P., Aphecetche, L. B., Appelshaeuser, H., Arcelli, S., Arnaldi,  
 564 R., Arnold, O. W., Arsene, I. C., Arslandok, M., Audurier, B., Augustinus, A., Averbek,  
 565 R. P., Azmi, M. D., Badala, A., Baek, Y. W., Bagnasco, S., Bailhache, R. M., Bala,  
 566 R., Balasubramanian, S., Baldisseri, A., Baral, R. C., Barbano, A. M., Barbera, R.,  
 567 Barile, F., Barnafoldi, G. G., Barnby, L. S., Ramillien Barret, V., Bartalini, P., Barth,  
 568 K., Bartke, J. G., Bartsch, E., Basile, M., Bastid, N., Basu, S., Bathen, B., Batigne,  
 569 G., Batista Camejo, A., Batyunya, B., Batzing, P. C., Bearden, I. G., Beck, H., Bedda,  
 570 C., Behera, N. K., Belikov, I., Bellini, F., Bello Martinez, H., Bellwied, R., Belmont Iii,  
 571 R. J., Belmont Moreno, E., Belyaev, V., Bencedi, G., Beole, S., Berceanu, I., Bercuci, A.,  
 572 Berdnikov, Y., Berenyi, D., Bertens, R. A., Berzano, D., Betev, L., Bhasin, A., Bhat, I. R.,  
 573 Bhati, A. K., Bhattacharjee, B., Bhom, J., Bianchi, L., Bianchi, N., Bianchin, C., Bielcik,  
 574 J., Bielcikova, J., Bilandzic, A., Biro, G., Biswas, R., Biswas, S., Bjelogrljic, S., Blair, J. T.,  
 575 Blau, D., Blume, C., Bock, F., Bogdanov, A., Boggild, H., Boldizar, L., Bombara, M.,  
 576 Book, J. H., Borel, H., Borissov, A., Borri, M., Bossu, F., Botta, E., Bourjau, C., Braun-  
 577 Munzinger, P., Bregant, M., Breitner, T. G., Broker, T. A., Browning, T. A., Broz, M.,  
 578 Brucken, E. J., Bruna, E., Bruno, G. E., Budnikov, D., Buesching, H., Bufalino, S., Buncic,  
 579 P., Busch, O., Buthelezi, E. Z., Bashir Butt, J., Buxton, J. T., Cabala, J., Caffarri, D.,  
 580 Cai, X., Caines, H. L., Calero Diaz, L., Caliva, A., Calvo Villar, E., Camerini, P., Carena,  
 581 F., Carena, W., Carnesecchi, F., Castillo Castellanos, J. E., Castro, A. J., Casula, E.  
 582 A. R., Ceballos Sanchez, C., Cepila, J., Cerello, P., Cerkala, J., Chang, B., Chapeland,  
 583 S., Chartier, M., Charvet, J.-L. F., Chattopadhyay, S., Chattopadhyay, S., Chauvin, A.,  
 584 Chelnokov, V., Cherney, M. G., Cheshkov, C. V., Cheynis, B., Chibante Barroso, V. M.,  
 585 Dobrigkeit Chinellato, D., Cho, S., Chochula, P., Choi, K., Chojnacki, M., Choudhury, S.,  
 586 Christakoglou, P., Christensen, C. H., Christiansen, P., Chujo, T., Chung, S.-U., Cicalo,  
 587 C., Cifarelli, L., Cindolo, F., Cleymans, J. W. A., Colamaria, F. F., Colella, D., Collu, A.,



588 Colocci, M., Conesa Balbastre, G., Conesa Del Valle, Z., Connors, M. E., Contreras Nuno,  
 589 J. G., Cormier, T. M., Corrales Morales, Y., Cortes Maldonado, I., Cortese, P., Cosentino,  
 590 M. R., Costa, F., Crochet, P., Cruz Albino, R., Cuautle Flores, E., Cunqueiro Mendez,  
 591 L., Dahms, T., Dainese, A., Danisch, M. C., Danu, A., Das, D., Das, I., Das, S., Dash,  
 592 A. K., Dash, S., De, S., De Caro, A., De Cataldo, G., De Conti, C., De Cuveland, J.,  
 593 De Falco, A., De Gruttola, D., De Marco, N., De Pasquale, S., Deisting, A., Deloff,  
 594 A., Denes, E. S., Deplano, C., Dhankher, P., Di Bari, D., Di Mauro, A., Di Nezza,  
 595 P., Diaz Corchero, M. A., Dietel, T., Dillenseger, P., Divia, R., Djuvsland, O., Dobrin,  
 596 A. F., Domenicis Gimenez, D., Donigus, B., Dordic, O., Drozhzhova, T., Dubey, A. K.,  
 597 Dubla, A., Ducroux, L., Dupieux, P., Ehlers Iii, R. J., Elia, D., Endress, E., Engel, H.,  
 598 Epple, E., Erasmus, B. E., Erdemir, I., Erhardt, F., Espagnon, B., Estienne, M. D.,  
 599 Esumi, S., Eum, J., Evans, D., Evdokimov, S., Eyyubova, G., Fabbietti, L., Fabris, D.,  
 600 Faivre, J., Fantoni, A., Fasel, M., Feldkamp, L., Feliciello, A., Feofilov, G., Ferencei, J.,  
 601 Fernandez Tellez, A., Gonzalez Ferreiro, E., Ferretti, A., Festanti, A., Feuillard, V. J. G.,  
 602 Figiel, J., Araujo Silva Figueredo, M., Filchagin, S., Finogeev, D., Fionda, F., Fiore, E. M.,  
 603 Fleck, M. G., Floris, M., Foertsch, S. V., Foka, P., Fokin, S., Fragiacomio, E., Francescon,  
 604 A., Frankenfeld, U. M., Fronze, G. G., Fuchs, U., Furget, C., Furs, A., Fusco Girard, M.,  
 605 Gaardhoeje, J. J., Gagliardi, M., Gago Medina, A. M., Gallio, M., Gangadharan, D. R.,  
 606 Ganoti, P., Gao, C., Garabatos Cuadrado, J., Garcia-Solis, E. J., Gargiulo, C., Gasik, P. J.,  
 607 Gauger, E. F., Germain, M., Gheata, M., Ghosh, P., Ghosh, S. K., Gianotti, P., Giubellino,  
 608 P., Giubilato, P., Gladysz-Dziadus, E., Glassel, P., Gomez Coral, D. M., Gomez Ramirez,  
 609 A., Sanchez Gonzalez, A., Gonzalez, V., Gonzalez Zamora, P., Gorbunov, S., Gorlich,  
 610 L. M., Gotovac, S., Grabski, V., Grachov, O. A., Graczykowski, L. K., Graham, K. L.,  
 611 Grelli, A., Grigoras, A. G., Grigoras, C., Grigoryev, V., Grigoryan, A., Grigoryan, S.,  
 612 Grynyov, B., Grion, N., Gronefeld, J. M., Grosse-Oetringhaus, J. F., Grosso, R., Guber,  
 613 F., Guernane, R., Guerzoni, B., Gulbrandsen, K. H., Gunji, T., Gupta, A., Gupta, R.,  
 614 Haake, R., Haaland, O. S., Hadjidakis, C. M., Haiduc, M., Hamagaki, H., Hamar, G.,  
 615 Hamon, J. C., Harris, J. W., Harton, A. V., Hatzifotiadou, D., Hayashi, S., Heckel, S. T.,  
 616 Hellbar, E., Helstrup, H., Herghelegiu, A. I., Herrera Corral, G. A., Hess, B. A., Hetland,  
 617 K. F., Hillemanns, H., Hippolyte, B., Horak, D., Hosokawa, R., Hristov, P. Z., Humanic,

618 T., Hussain, N., Hussain, T., Hutter, D., Hwang, D. S., Ilkaev, R., Inaba, M., Incani,  
 619 E., Ippolitov, M., Irfan, M., Ivanov, M., Ivanov, V., Izucheev, V., Jacazio, N., Jacobs,  
 620 P. M., Jadhav, M. B., Jadlovská, S., Jadlovsky, J., Jahnke, C., Jakubowska, M. J., Jang,  
 621 H. J., Janik, M. A., Pahula Hewage, S., Jena, C., Jena, S., Jimenez Bustamante, R. T.,  
 622 Jones, P. G., Jusko, A., Kalinak, P., Kalweit, A. P., Kamin, J. A., Kang, J. H., Kaplin,  
 623 V., Kar, S., Karasu Uysal, A., Karavichev, O., Karavicheva, T., Karayan, L., Karpechev,  
 624 E., Kebschull, U. W., Keidel, R., Keijden, D. L., Keil, M., Khan, M. M., Khan, P.,  
 625 Khan, S. A., Khanzadeev, A., Kharlov, Y., Kileng, B., Kim, D. W., Kim, D. J., Kim,  
 626 D., Kim, H., Kim, J., Kim, M., Kim, S. Y., Kim, T., Kirsch, S., Kisel, I., Kiselev,  
 627 S., Kisiel, A. R., Kiss, G., Klay, J. L., Klein, C., Klein, J., Klein-Boesing, C., Klewin,  
 628 S., Kluge, A., Knichel, M. L., Knospe, A. G., Kobdaj, C., Kofarago, M., Kollegger, T.,  
 629 Kolozhvari, A., Kondratev, V., Kondratyeva, N., Kondratyuk, E., Konevskikh, A., Kopicik,  
 630 M., Kostarakis, P., Kour, M., Kouzinopoulos, C., Kovalenko, O., Kovalenko, V., Kowalski,  
 631 M., Koyithatta Meethalevedu, G., Kralik, I., Kravcukova, A., Krivda, M., Krizek, F.,  
 632 Kryshen, E., Krzewicki, M., Kubera, A. M., Kucera, V., Kuhn, C. C., Kuijer, P. G.,  
 633 Kumar, A., Kumar, J., Kumar, L., Kumar, S., Kurashvili, P., Kurepin, A., Kurepin, A.,  
 634 Kuryakin, A., Kweon, M. J., Kwon, Y., La Pointe, S. L., La Rocca, P., Ladron De Guevara,  
 635 P., Lagana Fernandes, C., Lakomov, I., Langoy, R., Lapidus, K., Lara Martinez, C. E.,  
 636 Lardeux, A. X., Lattuca, A., Laudi, E., Lea, R., Leardini, L., Lee, G. R., Lee, S., Lehas, F.,  
 637 Lemmon, R. C., Lenti, V., Leogrande, E., Leon Monzon, I., Leon Vargas, H., Leoncino, M.,  
 638 Levai, P., Li, S., Li, X., Lien, J. A., Lietava, R., Lindal, S., Lindenstruth, V., Lippmann,  
 639 C., Lisa, M. A., Ljunggren, H. M., Lodato, D. F., Lonne, P.-I., Loginov, V., Loizides, C.,  
 640 Lopez, X. B., Lopez Torres, E., Lowe, A. J., Luettig, P. J., Lunardon, M., Luparello,  
 641 G., Lutz, T. H., Maevskaya, A., Mager, M., Mahajan, S., Mahmood, S. M., Maire,  
 642 A., Majka, R. D., Malaev, M., Maldonado Cervantes, I. A., Malinina, L., Mal'Kevich,  
 643 D., Malzacher, P., Mamonov, A., Manko, V., Manso, F., Manzari, V., Marchisone, M.,  
 644 Mares, J., Margagliotti, G. V., Margotti, A., Margutti, J., Marin, A. M., Markert, C.,  
 645 Marquard, M., Martin, N. A., Martin Blanco, J., Martinengo, P., Martinez Hernandez,  
 646 M. I., Martinez-Garcia, G., Martinez Pedreira, M., Mas, A. J.-M., Masciocchi, S., Masera,  
 647 M., Masoni, A., Mastroserio, A., Matyja, A. T., Mayer, C., Mazer, J. A., Mazzoni,

648 A. M., Mcdonald, D., Meddi, F., Melikyan, Y., Menchaca-Rocha, A. A., Meninno, E.,  
 649 Mercado-Perez, J., Meres, M., Miake, Y., Mieskolainen, M. M., Mikhaylov, K., Milano,  
 650 L., Milosevic, J., Mischke, A., Mishra, A. N., Miskowiec, D. C., Mitra, J., Mitu, C. M.,  
 651 Mohammadi, N., Mohanty, B., Molnar, L., Montano Zetina, L. M., Montes Prado, E.,  
 652 Moreira De Godoy, D. A., Perez Moreno, L. A., Moretto, S., Morreale, A., Morsch, A.,  
 653 Muccifora, V., Mudnic, E., Muhlheim, D. M., Muhuri, S., Mukherjee, M., Mulligan, J. D.,  
 654 Gameiro Munhoz, M., Munzer, R. H., Murakami, H., Murray, S., Musa, L., Musinsky,  
 655 J., Naik, B., Nair, R., Nandi, B. K., Nania, R., Nappi, E., Naru, M. U., Ferreira Natal  
 656 Da Luz, P. H., Nattrass, C., Rosado Navarro, S., Nayak, K., Nayak, R., Nayak, T. K.,  
 657 Nazarenko, S., Nedosekin, A., Nellen, L., Ng, F., Nicassio, M., Niculescu, M., Niedziela,  
 658 J., Nielsen, B. S., Nikolaev, S., Nikulin, S., Nikulin, V., Noferini, F., Nomokonov, P.,  
 659 Nooren, G., Cabanillas Noris, J. C., Norman, J., Nyanin, A., Nystrand, J. I., Oeschler,  
 660 H. O., Oh, S., Oh, S. K., Ohlson, A. E., Okatan, A., Okubo, T., Olah, L., Oleniacz,  
 661 J., Oliveira Da Silva, A. C., Oliver, M. H., Onderwaater, J., Oppedisano, C., Orava, R.,  
 662 Oravec, M., Ortiz Velasquez, A., Oskarsson, A. N. E., Otwinowski, J. T., Oyama, K.,  
 663 Ozdemir, M., Pachmayer, Y. C., Pagano, D., Pagano, P., Paic, G., Pal, S. K., Pan, J.,  
 664 Pandey, A. K., Papikyan, V., Pappalardo, G., Pareek, P., Park, W., Parmar, S., Passfeld,  
 665 A., Paticchio, V., Patra, R. N., Paul, B., Pei, H., Peitzmann, T., Pereira Da Costa, H.  
 666 D. A., Peresunko, D. Y., Perez Lara, C. E., Perez Lezama, E., Peskov, V., Pestov, Y.,  
 667 Petracek, V., Petrov, V., Petrovici, M., Petta, C., Piano, S., Pikna, M., Pillot, P., Ozelin  
 668 De Lima Pimentel, L., Pinazza, O., Pinsky, L., Piyrathna, D., Ploskon, M. A., Planinic,  
 669 M., Pluta, J. M., Pochybova, S., Podesta Lerma, P. L. M., Poghosyan, M., Polishchuk,  
 670 B., Poljak, N., Poonsawat, W., Pop, A., Porteboeuf, S. J., Porter, R. J., Pospisil, J.,  
 671 Prasad, S. K., Preghenella, R., Prino, F., Pruneau, C. A., Pshenichnov, I., Puccio, M.,  
 672 Puddu, G., Pujahari, P. R., Punin, V., Putschke, J. H., Qvigstad, H., Rachevski, A., Raha,  
 673 S., Rajput, S., Rak, J., Rakotozafindrabe, A. M., Ramello, L., Rami, F., Raniwala, R.,  
 674 Raniwala, S., Rasanen, S. S., Rascanu, B. T., Rathee, D., Read, K. F., Redlich, K., Reed,  
 675 R. J., Rehman, A. U., Reichelt, P. S., Reidt, F., Ren, X., Renfordt, R. A. E., Reolon, A. R.,  
 676 Reshetin, A., Reygers, K. J., Riabov, V., Ricci, R. A., Richert, T. O. H., Richter, M. R.,  
 677 Riedler, P., Riegler, W., Riggi, F., Ristea, C.-L., Rocco, E., Rodriguez Cahuantzi, M.,

678 Rodriguez Manso, A., Roeed, K., Rogochaya, E., Rohr, D. M., Roehrich, D., Ronchetti,  
 679 F., Ronflette, L., Rosnet, P., Rossi, A., Roukoutakis, F., Roy, A., Roy, C. S., Roy, P. K.,  
 680 Rubio Montero, A. J., Rui, R., Russo, R., Di Ruzza, B., Ryabinkin, E., Ryabov, Y.,  
 681 Rybicki, A., Saarinen, S., Sadhu, S., Sadovskiy, S., Safarik, K., Sahlmuller, B., Sahoo, P.,  
 682 Sahoo, R., Sahoo, S., Sahu, P. K., Saini, J., Sakai, S., Saleh, M. A., Salzwedel, J. S. N.,  
 683 Sambyal, S. S., Samsonov, V., Sandor, L., Sandoval, A., Sano, M., Sarkar, D., Sarkar, N.,  
 684 Sarma, P., Scapparone, E., Scarlassara, F., Schiaua, C. C., Schicker, R. M., Schmidt, C. J.,  
 685 Schmidt, H. R., Schuchmann, S., Schukraft, J., Schulc, M., Schutz, Y. R., Schwarz, K. E.,  
 686 Schweda, K. O., Scioli, G., Scomparin, E., Scott, R. M., Sefcik, M., Seger, J. E., Sekiguchi,  
 687 Y., Sekihata, D., Selyuzhenkov, I., Senosi, K., Senyukov, S., Serradilla Rodriguez, E.,  
 688 Sevcenco, A., Shabanov, A., Shabetai, A., Shadura, O., Shahoyan, R., Shahzad, M. I.,  
 689 Shangaraev, A., Sharma, A., Sharma, M., Sharma, M., Sharma, N., Sheikh, A. I., Shigaki,  
 690 K., Shou, Q., Shtejer Diaz, K., Sibiryak, Y., Siddhanta, S., Sielewicz, K. M., Siemiarczuk,  
 691 T., Silvermyr, D. O. R., Silvestre, C. M., Simatovic, G., Simonetti, G., Singaraju, R. N.,  
 692 Singh, R., Singha, S., Singhal, V., Sinha, B., Sarkar Sinha, T., Sitar, B., Sitta, M., Skaali,  
 693 B., Slupecki, M., Smirnov, N., Snellings, R., Snellman, T. W., Song, J., Song, M., Song,  
 694 Z., Soramel, F., Sorensen, S. P., Derradi De Souza, R., Sozzi, F., Spacek, M., Spiriti, E.,  
 695 Sputowska, I. A., Spyropoulou-Stassinaki, M., Stachel, J., Stan, I., Stankus, P., Stenlund,  
 696 E. A., Steyn, G. F., Stiller, J. H., Stocco, D., Strmen, P., Alarcon Do Passo Suaide, A.,  
 697 Sugitate, T., Suire, C. P., Suleymanov, M. K. O., Suljic, M., Sultanov, R., Sumbera,  
 698 M., Sumowidagdo, S., Szabo, A., Szanto De Toledo, A., Szarka, I., Szczepankiewicz, A.,  
 699 Szymanski, M. P., Tabassam, U., Takahashi, J., Tambave, G. J., Tanaka, N., Tarhini,  
 700 M., Tariq, M., Tarzila, M.-G., Tauro, A., Tejeda Munoz, G., Telesca, A., Terasaki, K.,  
 701 Terrevoli, C., Teyssier, B., Thaeder, J. M., Thakur, D., Thomas, D., Tieulent, R. N.,  
 702 Tikhonov, A., Timmins, A. R., Toia, A., Trogolo, S., Trombetta, G., Trubnikov, V.,  
 703 Trzaska, W. H., Tsuji, T., Tumkin, A., Turrisi, R., Tveter, T. S., Ullaland, K., Uras, A.,  
 704 Usai, G., Utrobicic, A., Vala, M., Valencia Palomo, L., Vallero, S., Van Der Maarel, J.,  
 705 Van Hoorne, J. W., Van Leeuwen, M., Vanat, T., Vande Vyvre, P., Varga, D., Diozcora  
 706 Vargas Trevino, A., Vargyas, M., Varma, R., Vasileiou, M., Vasiliev, A., Vauthier, A.,  
 707 Vazquez Doce, O., Vechernin, V., Veen, A. M., Veldhoen, M., Velure, A., Vercellin, E.,

Vergara Limon, S., Vernet, R., Verweij, M., Vickovic, L., Viinikainen, J. S., Vilakazi, Z.,  
Villalobos Baillie, O., Villatoro Tello, A., Vinogradov, A., Vinogradov, L., Vinogradov,  
Y., Virgili, T., Vislavicius, V., Viyogi, Y., Vodopyanov, A., Volkl, M. A., Voloshin, K.,  
Voloshin, S., Volpe, G., Von Haller, B., Vorobyev, I., Vranic, D., Vrlakova, J., Vulpescu,  
B., Wagner, B., Wagner, J., Wang, H., Wang, M., Watanabe, D., Watanabe, Y., Weber,  
M., Weber, S. G., Weiser, D. F., Wessels, J. P., Westerhoff, U., Whitehead, A. M.,  
Wiechula, J., Wikne, J., Wilk, G. A., Wilkinson, J. J., Williams, C., Windelband, B. S.,  
Winn, M. A., Yang, P., Yano, S., Yasin, Z., Yin, Z., Yokoyama, H., Yoo, I.-K., Yoon,  
J. H., Yurchenko, V., Yushmanov, I., Zaborowska, A., Zaccolo, V., Zaman, A., Zampolli,  
C., Correia Zanolini, H. J., Zaporozhets, S., Zardoshti, N., Zarochentsev, A., Zavada, P.,  
Zavvalov, N., Zbroszczyk, H. P., Zgura, S. I., Zhalov, M., Zhang, H., Zhang, X., Zhang,  
Y., Chunhui, Z., Zhang, Z., Zhao, C., Zhigareva, N., Zhou, D., Zhou, Y., Zhou, Z.,  
Zhu, H., Zhu, J., Zichichi, A., Zimmermann, A., Zimmermann, M. B., Zinovjev, G., and  
Zyzak, M. (2016). Measurement of transverse energy at midrapidity in Pb-Pb collisions at  
 $\sqrt{s_{NN}} = 2.76$  TeV. *Phys. Rev. C*, 94(CERN-EP-2016-071. CERN-EP-2016-071):034903.  
30 p. 30 pages, 14 captioned figures, 2 tables, authors from page 25, published version,  
figures at <http://aliceinfo.cern.ch/ArtSubmission/node/2400>. 6, 15

[2] Adamczyk, L., Adkins, J. K., Agakishiev, G., Aggarwal, M. M., Ahammed, Z., Ajitanand,  
N. N., Alekseev, I., Anderson, D. M., Aoyama, R., Aparin, A., Arkhipkin, D., Aschenauer,  
E. C., Ashraf, M. U., Attri, A., Averichev, G. S., Bai, X., Bairathi, V., Behera, A.,  
Bellwied, R., Bhasin, A., Bhati, A. K., Bhattarai, P., Bielcik, J., Bielcikova, J., Bland,  
L. C., Bordyuzhin, I. G., Bouchet, J., Brandenburg, J. D., Brandin, A. V., Brown, D.,  
Bunzarov, I., Butterworth, J., Caines, H., Calderón de la Barca Sánchez, M., Campbell,  
J. M., Cebra, D., Chakaberia, I., Chaloupka, P., Chang, Z., Chankova-Bunzarova, N.,  
Chatterjee, A., Chattopadhyay, S., Chen, X., Chen, J. H., Chen, X., Cheng, J., Cherney,  
M., Christie, W., Contin, G., Crawford, H. J., Das, S., De Silva, L. C., Debbe, R. R.,  
Dedovich, T. G., Deng, J., Derevschikov, A. A., Didenko, L., Dilks, C., Dong, X.,  
Drachenberg, J. L., Draper, J. E., Dunkelberger, L. E., Dunlop, J. C., Efimov, L. G.,  
Else, N., Engelage, J., Eppley, G., Esha, R., Esumi, S., Evdokimov, O., Ewigleben,

737 J., Eyser, O., Fatemi, R., Fazio, S., Federic, P., Federicova, P., Fedorisin, J., Feng, Z.,  
 738 Filip, P., Finch, E., Fisyak, Y., Flores, C. E., Fulek, L., Gagliardi, C. A., Garand, D.,  
 739 Geurts, F., Gibson, A., Girard, M., Grosnick, D., Gunarathne, D. S., Guo, Y., Gupta, A.,  
 740 Gupta, S., Guryn, W., Hamad, A. I., Hamed, A., Harlenderova, A., Harris, J. W., He, L.,  
 741 Heppelmann, S., Heppelmann, S., Hirsch, A., Hoffmann, G. W., Horvat, S., Huang, T.,  
 742 Huang, B., Huang, X., Huang, H. Z., Humanic, T. J., Huo, P., Igo, G., Jacobs, W. W.,  
 743 Jentsch, A., Jia, J., Jiang, K., Jowzaee, S., Judd, E. G., Kabana, S., Kalinkin, D., Kang,  
 744 K., Kauder, K., Ke, H. W., Keane, D., Kechechyan, A., Khan, Z., Kikoła, D. P., Kisel,  
 745 I., Kisiel, A., Kochenda, L., Kocmanek, M., Kollegger, T., Kosarzewski, L. K., Kraishan,  
 746 A. F., Kravtsov, P., Krueger, K., Kulathunga, N., Kumar, L., Kvapil, J., Kwasizur, J. H.,  
 747 Lacey, R., Landgraf, J. M., Landry, K. D., Lauret, J., Lebedev, A., Lednický, R., Lee,  
 748 J. H., Li, X., Li, C., Li, W., Li, Y., Lidrych, J., Lin, T., Lisa, M. A., Liu, H., Liu,  
 749 P., Liu, Y., Liu, F., Ljubicic, T., Llope, W. J., Lomnitz, M., Longacre, R. S., Luo, S.,  
 750 Luo, X., Ma, G. L., Ma, L., Ma, Y. G., Ma, R., Magdy, N., Majka, R., Mallick, D.,  
 751 Margetis, S., Markert, C., Matis, H. S., Meehan, K., Mei, J. C., Miller, Z. W., Minaev,  
 752 N. G., Mioduszewski, S., Mishra, D., Mizuno, S., Mohanty, B., Mondal, M. M., Morozov,  
 753 D. A., Mustafa, M. K., Nasim, M., Nayak, T. K., Nelson, J. M., Nie, M., Nigmatkulov,  
 754 G., Niida, T., Nogach, L. V., Nonaka, T., Nurushev, S. B., Odyniec, G., Ogawa, A.,  
 755 Oh, K., Okorokov, V. A., Olvitt, D., Page, B. S., Pak, R., Pandit, Y., Panebratsev, Y.,  
 756 Pawlik, B., Pei, H., Perkins, C., Pile, P., Pluta, J., Poniatowska, K., Porter, J., Posik,  
 757 M., Poskanzer, A. M., Pruthi, N. K., Przybycien, M., Putschke, J., Qiu, H., Quintero, A.,  
 758 Ramachandran, S., Ray, R. L., Reed, R., Rehbein, M. J., Ritter, H. G., Roberts, J. B.,  
 759 Rogachevskiy, O. V., Romero, J. L., Roth, J. D., Ruan, L., Rusnak, J., Rusnakova, O.,  
 760 Sahoo, N. R., Sahu, P. K., Salur, S., Sandweiss, J., Saur, M., Schambach, J., Schmäh,  
 761 A. M., Schmidke, W. B., Schmitz, N., Schweid, B. R., Seger, J., Sergeeva, M., Seyboth, P.,  
 762 Shah, N., Shahaliev, E., Shanmuganathan, P. V., Shao, M., Sharma, A., Sharma, M. K.,  
 763 Shen, W. Q., Shi, Z., Shi, S. S., Shou, Q. Y., Sichtermann, E. P., Sikora, R., Simko,  
 764 M., Singha, S., Skoby, M. J., Smirnov, N., Smirnov, D., Solyst, W., Song, L., Sorensen,  
 765 P., Spinka, H. M., Srivastava, B., Stanislaus, T. D. S., Strikhanov, M., Stringfellow, B.,  
 766 Sugiura, T., Sumbera, M., Summa, B., Sun, Y., Sun, X. M., Sun, X., Surrow, B., Svirida,

D. N., Tang, A. H., Tang, Z., Taranenko, A., Tarnowsky, T., Tawfik, A., Thäder, J., Thomas, J. H., Timmins, A. R., Tlusty, D., Todoroki, T., Tokarev, M., Trentalange, S., Tribble, R. E., Tribedy, P., Tripathy, S. K., Trzeciak, B. A., Tsai, O. D., Ullrich, T., Underwood, D. G., Upsal, I., Van Buren, G., van Nieuwenhuizen, G., Vasiliev, A. N., Videbæk, F., Vokal, S., Voloshin, S. A., Vossen, A., Wang, G., Wang, Y., Wang, F., Wang, Y., Webb, J. C., Webb, G., Wen, L., Westfall, G. D., Wieman, H., Wissink, S. W., Witt, R., Wu, Y., Xiao, Z. G., Xie, W., Xie, G., Xu, J., Xu, N., Xu, Q. H., Xu, Y. F., Xu, Z., Yang, Y., Yang, Q., Yang, C., Yang, S., Ye, Z., Ye, Z., Yi, L., Yip, K., Yoo, I.-K., Yu, N., Zbroszczyk, H., Zha, W., Zhang, Z., Zhang, X. P., Zhang, J. B., Zhang, S., Zhang, J., Zhang, Y., Zhang, J., Zhang, S., Zhao, J., Zhong, C., Zhou, L., Zhou, C., Zhu, X., Zhu, Z., and Zyzak, M. (2017). Bulk properties of the medium produced in relativistic heavy-ion collisions from the beam energy scan program. *Phys. Rev. C*, 96:044904. vii, 24, 28, 29

[3] Adare, A., Afanasiev, S., Aidala, C., Ajitanand, N. N., Akiba, Y., Akimoto, R., Al-Bataineh, H., Alexander, J., Alfred, M., Al-Jamel, A., Al-Ta'ani, H., Angerami, A., Aoki, K., Apadula, N., Aphecetche, L., Aramaki, Y., Armendariz, R., Aronson, S. H., Asai, J., Asano, H., Aschenauer, E. C., Atomssa, E. T., Auerbeck, R., Awes, T. C., Azmoun, B., Babintsev, V., Bai, M., Bai, X., Baksay, G., Baksay, L., Baldisseri, A., Bandara, N. S., Bannier, B., Barish, K. N., Barnes, P. D., Bassalleck, B., Basye, A. T., Bathe, S., Batsouli, S., Baublis, V., Bauer, F., Baumann, C., Baumgart, S., Bazilevsky, A., Beaumier, M., Beckman, S., Belikov, S., Belmont, R., Bennett, R., Berdnikov, A., Berdnikov, Y., Bhom, J. H., Bickley, A. A., Bjorndal, M. T., Black, D., Blau, D. S., Boissevain, J. G., Bok, J. S., Borel, H., Boyle, K., Brooks, M. L., Brown, D. S., Bryslawskyj, J., Bucher, D., Buesching, H., Bumazhnov, V., Bunce, G., Burward-Hoy, J. M., Butsyk, S., Campbell, S., Caringi, A., Castera, P., Chai, J.-S., Chang, B. S., Charvet, J.-L., Chen, C.-H., Chernichenko, S., Chi, C. Y., Chiba, J., Chiu, M., Choi, I. J., Choi, J. B., Choi, S., Choudhury, R. K., Christiansen, P., Chujo, T., Chung, P., Churn, A., Chvala, O., Cianciolo, V., Citron, Z., Cleven, C. R., Cobigo, Y., Cole, B. A., Comets, M. P., Conesa del Valle, Z., Connors, M., Constantin, P., Cronin, N., Crossette, N., Csanád, M., Csörgő, T., Dahms,

796 T., Dairaku, S., Danchev, I., Danley, T. W., Das, K., Datta, A., Daugherty, M. S.,  
 797 David, G., Dayananda, M. K., Deaton, M. B., DeBlasio, K., Dehmelt, K., Delagrange,  
 798 H., Denisov, A., d'Enterria, D., Deshpande, A., Desmond, E. J., Dharmawardane, K. V.,  
 799 Dietzsch, O., Ding, L., Dion, A., Diss, P. B., Do, J. H., Donadelli, M., D'Orazio, L.,  
 800 Drachenberg, J. L., Drapier, O., Drees, A., Drees, K. A., Dubey, A. K., Durham, J. M.,  
 801 Durum, A., Dutta, D., Dzhordzhadze, V., Edwards, S., Efremenko, Y. V., Egdemir, J.,  
 802 Ellinghaus, F., Emam, W. S., Engelmores, T., Enokizono, A., En'yo, H., Espagnon, B.,  
 803 Esumi, S., Eyser, K. O., Fadem, B., Feege, N., Fields, D. E., Finger, M., Finger, M.,  
 804 Fleuret, F., Fokin, S. L., Forestier, B., Fraenkel, Z., Frantz, J. E., Franz, A., Frawley,  
 805 A. D., Fujiwara, K., Fukao, Y., Fung, S.-Y., Fusayasu, T., Gadrat, S., Gainey, K., Gal,  
 806 C., Gallus, P., Garg, P., Garishvili, A., Garishvili, I., Gastineau, F., Ge, H., Germain, M.,  
 807 Giordano, F., Glenn, A., Gong, H., Gong, X., Gonin, M., Gosset, J., Goto, Y., Granier de  
 808 Cassagnac, R., Grau, N., Greene, S. V., Grim, G., Grosse Perdekamp, M., Gu, Y., Gunji,  
 809 T., Guo, L., Guragain, H., Gustafsson, H.-A., Hachiya, T., Hadj Henni, A., Haegemann,  
 810 C., Haggerty, J. S., Hagiwara, M. N., Hahn, K. I., Hamagaki, H., Hamblen, J., Hamilton,  
 811 H. F., Han, R., Han, S. Y., Hanks, J., Harada, H., Hartouni, E. P., Haruna, K., Harvey,  
 812 M., Hasegawa, S., Haseler, T. O. S., Hashimoto, K., Haslum, E., Hasuko, K., Hayano, R.,  
 813 Hayashi, S., He, X., Heffner, M., Hemmick, T. K., Hester, T., Heuser, J. M., Hiejima, H.,  
 814 Hill, J. C., Hobbs, R., Hohlmann, M., Hollis, R. S., Holmes, M., Holzmann, W., Homma,  
 815 K., Hong, B., Horaguchi, T., Hori, Y., Hornback, D., Hoshino, T., Hotvedt, N., Huang, J.,  
 816 Huang, S., Hur, M. G., Ichihara, T., Ichimiya, R., Iinuma, H., Ikeda, Y., Imai, K., Imazu,  
 817 Y., Imrek, J., Inaba, M., Inoue, Y., Iordanova, A., Isenhowe, D., Isenhowe, L., Ishihara,  
 818 M., Isinhue, A., Isobe, T., Issah, M., Isupov, A., Ivanishchev, D., Iwanaga, Y., Jacak,  
 819 B. V., Javani, M., Jeon, S. J., Jezghani, M., Jia, J., Jiang, X., Jin, J., Jinnouchi, O.,  
 820 Johnson, B. M., Jones, T., Joo, K. S., Jouan, D., Jumper, D. S., Kajihara, F., Kametani,  
 821 S., Kamihara, N., Kamin, J., Kanda, S., Kaneta, M., Kaneti, S., Kang, B. H., Kang, J. H.,  
 822 Kang, J. S., Kanou, H., Kapustinsky, J., Karatsu, K., Kasai, M., Kawagishi, T., Kawall,  
 823 D., Kawashima, M., Kazantsev, A. V., Kelly, S., Kempel, T., Key, J. A., Khachatryan, V.,  
 824 Khandai, P. K., Khanzadeev, A., Kijima, K. M., Kikuchi, J., Kim, A., Kim, B. I., Kim, C.,  
 825 Kim, D. H., Kim, D. J., Kim, E., Kim, E.-J., Kim, G. W., Kim, H. J., Kim, K.-B., Kim,



826 M., Kim, Y.-J., Kim, Y. K., Kim, Y.-S., Kimelman, B., Kinney, E., Kiss, A., Kistenev, E.,  
 827 Kitamura, R., Kiyomichi, A., Klatsky, J., Klay, J., Klein-Boesing, C., Kleinjan, D., Kline,  
 828 P., Koblesky, T., Kochenda, L., Kochetkov, V., Kofarago, M., Komatsu, Y., Komkov,  
 829 B., Konno, M., Koster, J., Kotchetkov, D., Kotov, D., Kozlov, A., Král, A., Kravitz, A.,  
 830 Krizek, F., Kroon, P. J., Kubart, J., Kunde, G. J., Kurihara, N., Kurita, K., Kurosawa,  
 831 M., Kweon, M. J., Kwon, Y., Kyle, G. S., Lacey, R., Lai, Y. S., Lajoie, J. G., Lebedev,  
 832 A., Le Bornec, Y., Leckey, S., Lee, B., Lee, D. M., Lee, G. H., Lee, J., Lee, K. B.,  
 833 Lee, K. S., Lee, M. K., Lee, S., Lee, S. H., Lee, S. R., Lee, T., Leitch, M. J., Leite, M.  
 834 A. L., Leitgab, M., Lenzi, B., Lewis, B., Li, X., Li, X. H., Lichtenwalner, P., Liebing, P.,  
 835 Lim, H., Lim, S. H., Linden Levy, L. A., Liška, T., Litvinenko, A., Liu, H., Liu, M. X.,  
 836 Love, B., Lynch, D., Maguire, C. F., Makdisi, Y. I., Makek, M., Malakhov, A., Malik,  
 837 M. D., Manion, A., Manko, V. I., Mannel, E., Mao, Y., Maruyama, T., Mašek, L., Masui,  
 838 H., Masumoto, S., Matathias, F., McCain, M. C., McCumber, M., McGaughey, P. L.,  
 839 McGlinchey, D., McKinney, C., Means, N., Meles, A., Mendoza, M., Meredith, B., Miake,  
 840 Y., Mibe, T., Midori, J., Mignerey, A. C., Mikeš, P., Miki, K., Miller, T. E., Milov, A.,  
 841 Mioduszewski, S., Mishra, D. K., Mishra, G. C., Mishra, M., Mitchell, J. T., Mitrovski,  
 842 M., Miyachi, Y., Miyasaka, S., Mizuno, S., Mohanty, A. K., Mohapatra, S., Montuenga,  
 843 P., Moon, H. J., Moon, T., Morino, Y., Morreale, A., Morrison, D. P., Moskowitz, M.,  
 844 Moss, J. M., Motschwiller, S., Moukhanova, T. V., Mukhopadhyay, D., Murakami, T.,  
 845 Murata, J., Mwai, A., Nagae, T., Nagamiya, S., Nagashima, K., Nagata, Y., Nagle, J. L.,  
 846 Naglis, M., Nagy, M. I., Nakagawa, I., Nakagomi, H., Nakamiya, Y., Nakamura, K. R.,  
 847 Nakamura, T., Nakano, K., Nam, S., Natrass, C., Nederlof, A., Netrakanti, P. K., Newby,  
 848 J., Nguyen, M., Nihashi, M., Niida, T., Nishimura, S., Norman, B. E., Nouicer, R., Novák,  
 849 T., Novitzky, N., Nukariya, A., Nyanin, A. S., Nystrand, J., Oakley, C., Obayashi, H.,  
 850 O'Brien, E., Oda, S. X., Ogilvie, C. A., Ohnishi, H., Oide, H., Ojha, I. D., Oka, M.,  
 851 Okada, K., Omiwade, O. O., Onuki, Y., Orjuela Koop, J. D., Osborn, J. D., Oskarsson,  
 852 A., Otterlund, I., Ouchida, M., Ozawa, K., Pak, R., Pal, D., Palounek, A. P. T., Pantuev,  
 853 V., Papavassiliou, V., Park, B. H., Park, I. H., Park, J., Park, J. S., Park, S., Park, S. K.,  
 854 Park, W. J., Pate, S. F., Patel, L., Patel, M., Pei, H., Peng, J.-C., Pereira, H., Perepelitsa,  
 855 D. V., Perera, G. D. N., Peresedov, V., Peressounko, D., Perry, J., Petti, R., Pinkenburg,

856 C., Pinson, R., Pisani, R. P., Proissl, M., Purschke, M. L., Purwar, A. K., Qu, H., Rak,  
 857 J., Rakotozafindrabe, A., Ramson, B. J., Ravinovich, I., Read, K. F., Rembeczki, S.,  
 858 Reuter, M., Reygers, K., Reynolds, D., Riabov, V., Riabov, Y., Richardson, E., Rinn, T.,  
 859 Riveli, N., Roach, D., Roche, G., Rolnick, S. D., Romana, A., Rosati, M., Rosen, C. A.,  
 860 Rosendahl, S. S. E., Rosnet, P., Rowan, Z., Rubin, J. G., Rukoyatkin, P., Ružička, P.,  
 861 Rykov, V. L., Ryu, M. S., Ryu, S. S., Sahlmueller, B., Saito, N., Sakaguchi, T., Sakai, S.,  
 862 Sakashita, K., Sakata, H., Sako, H., Samsonov, V., Sano, M., Sano, S., Sarsour, M., Sato,  
 863 H. D., Sato, S., Sato, T., Sawada, S., Schaefer, B., Schmoll, B. K., Sedgwick, K., Seele,  
 864 J., Seidl, R., Sekiguchi, Y., Semenov, V., Sen, A., Seto, R., Sett, P., Sexton, A., Sharma,  
 865 D., Shaver, A., Shea, T. K., Shein, I., Shevel, A., Shibata, T.-A., Shigaki, K., Shimomura,  
 866 M., Shohjoh, T., Shoji, K., Shukla, P., Sickles, A., Silva, C. L., Silvermyr, D., Silvestre,  
 867 C., Sim, K. S., Singh, B. K., Singh, C. P., Singh, V., Skolnik, M., Skutnik, S., Slunečka,  
 868 M., Smith, W. C., Snowball, M., Solano, S., Soldatov, A., Soltz, R. A., Sondheim, W. E.,  
 869 Sorensen, S. P., Sourikova, I. V., Staley, F., Stankus, P. W., Steinberg, P., Stenlund, E.,  
 870 Stepanov, M., Ster, A., Stoll, S. P., Stone, M. R., Sugitate, T., Suire, C., Sukhanov, A.,  
 871 Sullivan, J. P., Sumita, T., Sun, J., Sziklai, J., Tabaru, T., Takagi, S., Takagui, E. M.,  
 872 Takahara, A., Taketani, A., Tanabe, R., Tanaka, K. H., Tanaka, Y., Taneja, S., Tanida, K.,  
 873 Tannenbaum, M. J., Tarafdar, S., Taranenko, A., Tarján, P., Tennant, E., Themann, H.,  
 874 Thomas, D., Thomas, T. L., Tieulent, R., Timilsina, A., Todoroki, T., Togawa, M., Toia,  
 875 A., Tojo, J., Tomášek, L., Tomášek, M., Torii, H., Towell, C. L., Towell, R., Towell, R. S.,  
 876 Tram, V.-N., Tserruya, I., Tsuchimoto, Y., Tsuji, T., Tuli, S. K., Tydesjö, H., Tyurin,  
 877 N., Vale, C., Valle, H., van Hecke, H. W., Vargyas, M., Vazquez-Zambrano, E., Veicht,  
 878 A., Velkovska, J., Vértési, R., Vinogradov, A. A., Virius, M., Voas, B., Vossen, A., Vrba,  
 879 V., Vznuzdaev, E., Wagner, M., Walker, D., Wang, X. R., Watanabe, D., Watanabe, K.,  
 880 Watanabe, Y., Watanabe, Y. S., Wei, F., Wei, R., Wessels, J., Whitaker, S., White, A. S.,  
 881 White, S. N., Willis, N., Winter, D., Wolin, S., Woody, C. L., Wright, R. M., Wysocki, M.,  
 882 Xia, B., Xie, W., Xue, L., Yalcin, S., Yamaguchi, Y. L., Yamaura, K., Yang, R., Yanovich,  
 883 A., Yasin, Z., Ying, J., Yokkaichi, S., Yoo, J. H., Yoon, I., You, Z., Young, G. R., Younus,  
 884 I., Yu, H., Yushmanov, I. E., Zajc, W. A., Zaudtke, O., Zelenski, A., Zhang, C., Zhou, S.,

Zimanyi, J., Zolin, L., and Zou, L. (2016). Transverse energy production and charged-particle multiplicity at midrapidity in various systems from  $\sqrt{s_{NN}} = 7.7$  to 200 gev. *Phys. Rev. C*, 93:024901. 5, 28

[4] Adare, A., Afanasiev, S., Aidala, C., Ajitanand, N. N., Akiba, Y., Al-Bataineh, H., Alexander, J., Al-Jamel, A., Aoki, K., Aphecetche, L., and et al. (2007). Scaling Properties of Azimuthal Anisotropy in Au+Au and Cu+Cu Collisions at  $s_{NN}=200\text{GeV}$ . *Physical Review Letters*, 98(16):162301. vi, 16, 17, 18

[5] Adler, S. S., Afanasiev, S., Aidala, C., Ajitanand, N. N., Akiba, Y., Al-Jamel, A., Alexander, J., Aoki, K., Aphecetche, L., Armendariz, R., Aronson, S. H., Auerbeck, R., Awes, T. C., Azmoun, B., Babintsev, V., Baldisseri, A., Barish, K. N., Barnes, P. D., Bassalleck, B., Bathe, S., Batsouli, S., Baublis, V., Bauer, F., Bazilevsky, A., Belikov, S., Bennett, R., Berdnikov, Y., Bjorndal, M. T., Boissevain, J. G., Borel, H., Boyle, K., Brooks, M. L., Brown, D. S., Bruner, N., Bucher, D., Buesching, H., Bumazhnov, V., Bunce, G., Burward-Hoy, J. M., Butsyk, S., Camard, X., Campbell, S., Chai, J.-S., Chand, P., Chang, W. C., Chernichenko, S., Chi, C. Y., Chiba, J., Chiu, M., Choi, I. J., Choudhury, R. K., Chujo, T., Cianciolo, V., Cleven, C. R., Cobigo, Y., Cole, B. A., Comets, M. P., Constantin, P., Csanád, M., Csörgő, T., Cussonneau, J. P., Dahms, T., Das, K., David, G., Deák, F., Delagrange, H., Denisov, A., d'Enterria, D., Deshpande, A., Desmond, E. J., Devismes, A., Dietzsch, O., Dion, A., Drachenberg, J. L., Drapier, O., Drees, A., Dubey, A. K., Durum, A., Dutta, D., Dzhordzhadze, V., Efremenko, Y. V., Egdemir, J., Enokizono, A., En'yo, H., Espagnon, B., Esumi, S., Fields, D. E., Finck, C., Fleuret, F., Fokin, S. L., Forestier, B., Fox, B. D., Fraenkel, Z., Frantz, J. E., Franz, A., Frawley, A. D., Fukao, Y., Fung, S.-Y., Gadrat, S., Gastineau, F., Germain, M., Glenn, A., Gonin, M., Gosset, J., Goto, Y., Granier de Cassagnac, R., Grau, N., Greene, S. V., Grosse Perdekamp, M., Gunji, T., Gustafsson, H.-A., Hachiya, T., Hadj Henni, A., Haggerty, J. S., Hagiwara, M. N., Hamagaki, H., Hansen, A. G., Harada, H., Hartouni, E. P., Haruna, K., Harvey, M., Haslum, E., Hasuko, K., Hayano, R., He, X., Heffner, M., Hemmick, T. K., Heuser, J. M., Hidas, P., Hiejima, H., Hill, J. C., Hobbs, R., Holmes, M., Holzmann, W., Homma, K., Hong, B., Hoover, A., Horaguchi, T., Hur, M. G., Ichihara, T.,

914 Iinuma, H., Ikonnikov, V. V., Imai, K., Inaba, M., Inuzuka, M., Isenhowe, D., Isenhowe,  
 915 L., Ishihara, M., Isobe, T., Issah, M., Isupov, A., Jacak, B. V., Jia, J., Jin, J., Jinnouchi,  
 916 O., Johnson, B. M., Johnson, S. C., Joo, K. S., Jouan, D., Kajihara, F., Kametani,  
 917 S., Kamihara, N., Kaneta, M., Kang, J. H., Katou, K., Kawabata, T., Kawagishi, T.,  
 918 Kazantsev, A. V., Kelly, S., Khachaturov, B., Khanzadeev, A., Kikuchi, J., Kim, D. J.,  
 919 Kim, E., Kim, E. J., Kim, G.-B., Kim, H. J., Kim, Y.-S., Kinney, E., Kiss, A., Kistenev, E.,  
 920 Kiyomichi, A., Klein-Boesing, C., Kobayashi, H., Kochenda, L., Kochetkov, V., Kohara,  
 921 R., Komkov, B., Konno, M., Kotchetkov, D., Kozlov, A., Kroon, P. J., Kuberg, C. H.,  
 922 Kunde, G. J., Kurihara, N., Kurita, K., Kweon, M. J., Kwon, Y., Kyle, G. S., Lacey, R.,  
 923 Lajoie, J. G., Lebedev, A., Le Bornec, Y., Leckey, S., Lee, D. M., Lee, M. K., Leitch,  
 924 M. J., Leite, M. A. L., Li, X. H., Lim, H., Litvinenko, A., Liu, M. X., Maguire, C. F.,  
 925 Makdisi, Y. I., Malakhov, A., Malik, M. D., Manko, V. I., Mao, Y., Martinez, G., Masui,  
 926 H., Matathias, F., Matsumoto, T., McCain, M. C., McGaughey, P. L., Miake, Y., Miller,  
 927 T. E., Milov, A., Mioduszewski, S., Mishra, G. C., Mitchell, J. T., Mohanty, A. K.,  
 928 Morrison, D. P., Moss, J. M., Moukhanova, T. V., Mukhopadhyay, D., Muniruzzaman,  
 929 M., Murata, J., Nagamiya, S., Nagata, Y., Nagle, J. L., Naglis, M., Nakamura, T., Newby,  
 930 J., Nguyen, M., Norman, B. E., Nyanin, A. S., Nystrand, J., O'Brien, E., Ogilvie, C. A.,  
 931 Ohnishi, H., Ojha, I. D., Okada, K., Omiwade, O. O., Oskarsson, A., Otterlund, I., Oyama,  
 932 K., Ozawa, K., Pal, D., Palounek, A. P. T., Pantuev, V., Papavassiliou, V., Park, J., Park,  
 933 W. J., Pate, S. F., Pei, H., Penev, V., Peng, J.-C., Pereira, H., Peresedov, V., Peressounko,  
 934 D., Pierson, A., Pinkenburg, C., Pisani, R. P., Purschke, M. L., Purwar, A. K., Qu, H.,  
 935 Qualls, J. M., Rak, J., Ravinovich, I., Read, K. F., Reuter, M., Reygers, K., Riabov,  
 936 V., Riabov, Y., Roche, G., Romana, A., Rosati, M., Rosendahl, S. S. E., Rosnet, P.,  
 937 Rukoyatkin, P., Rykov, V. L., Ryu, S. S., Sahlmueller, B., Saito, N., Sakaguchi, T., Sakai,  
 938 S., Samsonov, V., Sanfratello, L., Santo, R., Sarsour, M., Sato, H. D., Sato, S., Sawada,  
 939 S., Schutz, Y., Semenov, V., Seto, R., Sharma, D., Shea, T. K., Shein, I., Shibata, T.-A.,  
 940 Shigaki, K., Shimomura, M., Shohjoh, T., Shoji, K., Sickles, A., Silva, C. L., Silvermyr, D.,  
 941 Sim, K. S., Singh, C. P., Singh, V., Skutnik, S., Smith, W. C., Soldatov, A., Soltz, R. A.,  
 942 Sondheim, W. E., Sorensen, S. P., Sourikova, I. V., Staley, F., Stankus, P. W., Stenlund,  
 943 E., Stepanov, M., Ster, A., Stoll, S. P., Sugitate, T., Suire, C., Sullivan, J. P., Sziklai, J.,

944 Tabaru, T., Takagi, S., Takagui, E. M., Taketani, A., Tanaka, K. H., Tanaka, Y., Tanida,  
 945 K., Tannenbaum, M. J., Taranenko, A., Tarján, P., Thomas, T. L., Togawa, M., Tojo, J.,  
 946 Torii, H., Towell, R. S., Tram, V.-N., Tserruya, I., Tsuchimoto, Y., Tuli, S. K., Tydesjö,  
 947 H., Tyurin, N., Uam, T. J., Vale, C., Valle, H., van Hecke, H. W., Velkovska, J., Velkovsky,  
 948 M., Vértesi, R., Veszprémi, V., Vinogradov, A. A., Volkov, M. A., Vznuzdaev, E., Wagner,  
 949 M., Wang, X. R., Watanabe, Y., Wessels, J., White, S. N., Willis, N., Winter, D., Wohn,  
 950 F. K., Woody, C. L., Wysocki, M., Xie, W., Yanovich, A., Yokkaichi, S., Young, G. R.,  
 951 Younus, I., Yushmanov, I. E., Zajc, W. A., Zaudtke, O., Zhang, C., Zhou, S., Zimányi, J.,  
 952 Zolin, L., and Zong, X. (2014). Transverse-energy distributions at midrapidity in  $p + p$ ,  
 953  $d + \text{Au}$ , and  $\text{Au} + \text{Au}$  collisions at  $\sqrt{s_{\text{NN}}} = 62.4 \sim 200$  gev and implications for particle-  
 954 production models. *Phys. Rev. C*, 89:044905. 22

955 [6] Adler, S. S., Afanasiev, S., Aidala, C., Ajitanand, N. N., Akiba, Y., Alexander, J.,  
 956 Amirikas, R., Aphecetche, L., Aronson, S. H., Auerbeck, R., Awes, T. C., Azmoun, R.,  
 957 Babintsev, V., Baldissieri, A., Barish, K. N., Barnes, P. D., Bassalleck, B., Bathe, S.,  
 958 Batsouli, S., Baublis, V., Bazilevsky, A., Belikov, S., Berdnikov, Y., Bhagavatula, S.,  
 959 Boissevain, J. G., Borel, H., Borenstein, S., Brooks, M. L., Brown, D. S., Bruner, N.,  
 960 Bucher, D., Buesching, H., Bumazhnov, V., Bunce, G., Burward-Hoy, J. M., Butsyk, S.,  
 961 Camard, X., Chai, J.-S., Chand, P., Chang, W. C., Chernichenko, S., Chi, C. Y., Chiba,  
 962 J., Chiu, M., Choi, I. J., Choi, J., Choudhury, R. K., Chujo, T., Cianciolo, V., Cobigo,  
 963 Y., Cole, B. A., Constantin, P., d’Enterria, D. G., David, G., Delagrange, H., Denisov, A.,  
 964 Deshpande, A., Desmond, E. J., Dietzsch, O., Drapier, O., Drees, A., Rietz, R. d., Durum,  
 965 A., Dutta, D., Efremenko, Y. V., Chenawi, K. E., Enokizono, A., En’yo, H., Esumi,  
 966 S., Ewell, L., Fields, D. E., Fleuret, F., Fokin, S. L., Fox, B. D., Fraenkel, Z., Frantz,  
 967 J. E., Franz, A., Frawley, A. D., Fung, S.-Y., Garpman, S., Ghosh, T. K., Glenn, A.,  
 968 Gogiberidze, G., Gonin, M., Gosset, J., Goto, Y., Cassagnac, R. G. d., Grau, N., Greene,  
 969 S. V., Perdekamp, M. G., Guryn, W., Gustafsson, H.-A., Hachiya, T., Haggerty, J. S.,  
 970 Hamagaki, H., Hansen, A. G., Hartouni, E. P., Harvey, M., Hayano, R., He, X., Heffner,  
 971 M., Hemmick, T. K., Heuser, J. M., Hibino, M., Hill, J. C., Holzmann, W., Homma, K.,  
 972 Hong, B., Hoover, A., Ichihara, T., Ikonnikov, V. V., Imai, K., Isenhower, D., Ishihara,

973 M., Issah, M., Isupov, A., Jacak, B. V., Jang, W. Y., Jeong, Y., Jia, J., Jinnouchi, O.,  
 974 Johnson, B. M., Johnson, S. C., Joo, K. S., Jouan, D., Kametani, S., Kamihara, N.,  
 975 Kang, J. H., Kapoor, S. S., Katou, K., Kelly, S., Khachaturov, B., Khanzadeev, A.,  
 976 Kikuchi, J., Kim, D. H., Kim, D. J., Kim, D. W., Kim, E., Kim, G.-B., Kim, H. J.,  
 977 Kistenev, E., Kiyomichi, A., Kiyoyama, K., Klein-Boesing, C., Kobayashi, H., Kochenda,  
 978 L., Kochetkov, V., Koehler, D., Kohama, T., Kopytine, M., Kotchetkov, D., Kozlov, A.,  
 979 Kroon, P. J., Kuberg, C. H., Kurita, K., Kuroki, Y., Kweon, M. J., Kwon, Y., Kyle,  
 980 G. S., Lacey, R., Ladygin, V., Lajoie, J. G., Lebedev, A., Leckey, S., Lee, D. M., Lee, S.,  
 981 Leitch, M. J., Li, X. H., Lim, H., Litvinenko, A., Liu, M. X., Liu, Y., Maguire, C. F.,  
 982 Makdisi, Y. I., Malakhov, A., Manko, V. I., Mao, Y., Martinez, G., Marx, M. D., Masui,  
 983 H., Matathias, F., Matsumoto, T., McGaughey, P. L., Melnikov, E., Mendenhall, M.,  
 984 Messer, F., Miake, Y., Milan, J., Miller, T. E., Milov, A., Mioduszewski, S., Mischke,  
 985 R. E., Mishra, G. C., Mitchell, J. T., Mohanty, A. K., Morrison, D. P., Moss, J. M.,  
 986 Mühlbacher, F., Mukhopadhyay, D., Muniruzzaman, M., Murata, J., Nagamiya, S., Nagle,  
 987 J. L., Nakamura, T., Nandi, B. K., Nara, M., Newby, J., Nilsson, P., Nyanin, A. S.,  
 988 Nystrand, J., O'Brien, E., Ogilvie, C. A., Ohnishi, H., Ojha, I. D., Okada, K., Ono, M.,  
 989 Onuchin, V., Oskarsson, A., Otterlund, I., Oyama, K., Ozawa, K., Pal, D., Palounek, A.  
 990 P. T., Pantuev, V. S., Papavassiliou, V., Park, J., Parmar, A., Pate, S. F., Peitzmann,  
 991 T., Peng, J.-C., Peresedov, V., Pinkenburg, C., Pisani, R. P., Plasil, F., Purschke, M. L.,  
 992 Purwar, A. K., Rak, J., Ravinovich, I., Read, K. F., Reuter, M., Reygers, K., Riabov, V.,  
 993 Riabov, Y., Roche, G., Romana, A., Rosati, M., Rosnet, P., Ryu, S. S., Sadler, M. E.,  
 994 Saito, N., Sakaguchi, T., Sakai, M., Sakai, S., Samsonov, V., Sanfratello, L., Santo, R.,  
 995 Sato, H. D., Sato, S., Sawada, S., Schutz, Y., Semenov, V., Seto, R., Shaw, M. R., Shea,  
 996 T. K., Shibata, T.-A., Shigaki, K., Shiina, T., Silva, C. L., Silvermyr, D., Sim, K. S., Singh,  
 997 C. P., Singh, V., Sivertz, M., Soldatov, A., Soltz, R. A., Sondheim, W. E., Sorensen, S. P.,  
 998 Sourikova, I. V., Staley, F., Stankus, P. W., Stenlund, E., Stepanov, M., Ster, A., Stoll,  
 999 S. P., Sugitate, T., Sullivan, J. P., Takagui, E. M., Taketani, A., Tamai, M., Tanaka, K. H.,  
 1000 Tanaka, Y., Tanida, K., Tannenbaum, M. J., Tarján, P., Tepe, J. D., Thomas, T. L., Tojo,  
 1001 J., Torii, H., Towell, R. S., Tserruya, I., Tsuruoka, H., Tuli, S. K., Tydesjö, H., Tyurin,  
 1002 N., Hecke, H. W. v., Velkovska, J., Velkovsky, M., Villatte, L., Vinogradov, A. A., Volkov,

M. A., Vznuzdaev, E., Wang, X. R., Watanabe, Y., White, S. N., Wohn, F. K., Woody, C. L., Xie, W., Yang, Y., Yanovich, A., Yokkaichi, S., Young, G. R., Yushmanov, I. E., Zajc, W. A., Zhang, C., Zhou, S., Zhou, S. J., and Zolin, L. (2005). Systematic studies of the centrality and  $\sqrt{s_{NN}}$  dependence of the  $de_T/d\eta$  and  $dn_{ch}/d\eta$  in heavy ion collisions at midrapidity. *Phys. Rev. C*, 71:034908. 23

[7] Anderson, M. et al. (2003). The Star time projection chamber: A Unique tool for studying high multiplicity events at RHIC. *Nucl. Instrum. Meth.*, A499:659–678. 26

[8] Ayala, A. (2016). Hadronic matter at the edge: A survey of some theoretical approaches to the physics of the qcd phase diagram. *Journal of Physics: Conference Series*, 761(1):012066. vi, 5, 6

[9] Bethe, H. A. and Ashkin, J. (1953). Passage of radiations through matter experimental nuclear physics vol 1 ed e segre. 24

[10] Bjorken, J. D. (1983). Highly relativistic nucleus-nucleus collisions: The central rapidity region. *Phys. Rev. D*, 27:140–151. 15

[11] Chatrchyan, S., Khachatryan, V., Sirunyan, A. M., Tumasyan, A., Adam, W., Bergauer, T., Dragicevic, M., Erö, J., Fabjan, C., Friedl, M., Frühwirth, R., Ghete, V. M., Hammer, J., Hörmann, N., Hrubec, J., Jeitler, M., Kiesenhofer, W., Knünz, V., Krammer, M., Liko, D., Mikulec, I., Pernicka, M., Rahbaran, B., Rohringer, C., Rohringer, H., Schöfbeck, R., Strauss, J., Taurok, A., Wagner, P., Waltenberger, W., Walzel, G., Widl, E., Wulz, C.-E., Mossolov, V., Shumeiko, N., Suarez Gonzalez, J., Bansal, S., Cornelis, T., De Wolf, E. A., Janssen, X., Luyckx, S., Maes, T., Mucibello, L., Ochesanu, S., Roland, B., Rougny, R., Selvaggi, M., Staykova, Z., Van Haeve, H., Van Mechelen, P., Van Remortel, N., Van Spilbeeck, A., Blekman, F., Blyweert, S., D’Hondt, J., Gonzalez Suarez, R., Kalogeropoulos, A., Maes, M., Olbrechts, A., Van Doninck, W., Van Mulders, P., Van Onsem, G. P., Vilella, I., Clerbaux, B., De Lentdecker, G., Dero, V., Gay, A. P. R., Hreus, T., Léonard, A., Marage, P. E., Reis, T., Thomas, L., Vander Velde, C., Vanlaer, P., Wang, J., Adler, V., Beernaert, K., Cimmino, A., Costantini, S., Garcia, G., Grunewald, M., Klein, B., Lellouch, J., Marinov, A., McCartin, J., Ocampo Rios, A. A., Ryckbosch, D.,

1031 Strobbe, N., Thyssen, F., Tytgat, M., Verwilligen, P., Walsh, S., Yazgan, E., Zaganidis,  
 1032 N., Basegmez, S., Bruno, G., Castello, R., Ceard, L., Delaere, C., du Pree, T., Favart, D.,  
 1033 Forthomme, L., Giammanco, A., Hollar, J., Lemaitre, V., Liao, J., Militaru, O., Nuttens,  
 1034 C., Pagano, D., Pin, A., Piotrkowski, K., Schul, N., Vizan Garcia, J. M., Beliy, N.,  
 1035 Caebergs, T., Daubie, E., Hammad, G. H., Alves, G. A., Correa Martins Junior, M.,  
 1036 De Jesus Damiao, D., Martins, T., Pol, M. E., Souza, M. H. G., Aldá Júnior, W. L.,  
 1037 Carvalho, W., Custódio, A., Da Costa, E. M., De Oliveira Martins, C., Fonseca De Souza,  
 1038 S., Matos Figueiredo, D., Mundim, L., Nogima, H., Oguri, V., Prado Da Silva, W. L.,  
 1039 Santoro, A., Soares Jorge, L., Sznajder, A., Bernardes, C. A., Dias, F. A., Fernandez  
 1040 Perez Tomei, T. R., Gregores, E. M., Lagana, C., Marinho, F., Mercadante, P. G., Novaes,  
 1041 S. F., Padula, S. S., Genchev, V., Iaydjiev, P., Piperov, S., Rodozov, M., Stoykova, S.,  
 1042 Sultanov, G., Tcholakov, V., Trayanov, R., Vutova, M., Dimitrov, A., Hadjiiska, R.,  
 1043 Kozhuharov, V., Litov, L., Pavlov, B., Petkov, P., Bian, J. G., Chen, G. M., Chen, H. S.,  
 1044 Jiang, C. H., Liang, D., Liang, S., Meng, X., Tao, J., Wang, J., Wang, X., Wang, Z.,  
 1045 Xiao, H., Xu, M., Zang, J., Zhang, Z., Asawatangtrakuldee, C., Ban, Y., Guo, S., Guo,  
 1046 Y., Li, W., Liu, S., Mao, Y., Qian, S. J., Teng, H., Wang, S., Zhu, B., Zou, W., Avila,  
 1047 C., Gomez, J. P., Gomez Moreno, B., Osorio Oliveros, A. F., Sanabria, J. C., Godinovic,  
 1048 N., Lelas, D., Plestina, R., Polic, D., Puljak, I., Antunovic, Z., Kovac, M., Brigljevic, V.,  
 1049 Duric, S., Kadija, K., Luetic, J., Morovic, S., Attikis, A., Galanti, M., Mavromanolakis,  
 1050 G., Mousa, J., Nicolaou, C., Ptochos, F., Razis, P. A., Finger, M., Finger, M., Assran,  
 1051 Y., Elgammal, S., Ellithi Kamel, A., Khalil, S., Mahmoud, M. A., Radi, A., Kadastik,  
 1052 M., Müntel, M., Raidal, M., Rebane, L., Tiko, A., Azzolini, V., Eerola, P., Fedi, G.,  
 1053 Voutilainen, M., Härkönen, J., Heikkinen, A., Karimäki, V., Kinnunen, R., Kortelainen,  
 1054 M. J., Lampén, T., Lassila-Perini, K., Lehti, S., Lindén, T., Luukka, P., Mäenpää, T.,  
 1055 Peltola, T., Tuominen, E., Tuominiemi, J., Tuovinen, E., Ungaro, D., Wendland, L.,  
 1056 Banzuzi, K., Karjalainen, A., Korpela, A., Tuuva, T., Besancon, M., Choudhury, S.,  
 1057 Dejardin, M., Denegri, D., Fabbro, B., Faure, J. L., Ferri, F., Ganjour, S., Givernaud,  
 1058 A., Gras, P., Hamel de Monchenault, G., Jarry, P., Locci, E., Malcles, J., Millischer, L.,  
 1059 Nayak, A., Rander, J., Rosowsky, A., Shreyber, I., Titov, M., Baffioni, S., Beaudette,  
 1060 F., Benhabib, L., Bianchini, L., Bluj, M., Broutin, C., Busson, P., Charlot, C., Daci,



1061 N., Dahms, T., Dobrzynski, L., Granier de Cassagnac, R., Haguenauer, M., Miné, P.,  
 1062 Mironov, C., Nguyen, M., Ochando, C., Paganini, P., Sabes, D., Salerno, R., Sirois, Y.,  
 1063 Veelken, C., Zabi, A., Agram, J.-L., Andrea, J., Bloch, D., Bodin, D., Brom, J.-M.,  
 1064 Cardaci, M., Chabert, E. C., Collard, C., Conte, E., Drouhin, F., Ferro, C., Fontaine, J.-  
 1065 C., Gelé, D., Goerlach, U., Juillot, P., Le Bihan, A.-C., Van Hove, P., Fassi, F., Mercier,  
 1066 D., Beauceron, S., Beaupere, N., Bondu, O., Boudoul, G., Chasserat, J., Chierici, R.,  
 1067 Contardo, D., Depasse, P., El Mamouni, H., Fay, J., Gascon, S., Gouzevitch, M., Ille,  
 1068 B., Kurca, T., Lethuillier, M., Mirabito, L., Perries, S., Sordini, V., Tosi, S., Tschudi,  
 1069 Y., Verdier, P., Viret, S., Tsamalaidze, Z., Anagnostou, G., Beranek, S., Edelhoff, M.,  
 1070 Feld, L., Heracleous, N., Hindrichs, O., Jussen, R., Klein, K., Merz, J., Ostapchuk, A.,  
 1071 Perieanu, A., Raupach, F., Sammet, J., Schael, S., Sprenger, D., Weber, H., Wittmer,  
 1072 B., Zhukov, V., Ata, M., Caudron, J., Dietz-Laursonn, E., Erdmann, M., Güth, A.,  
 1073 Hebbeker, T., Heidemann, C., Hoepfner, K., Klingebiel, D., Kreuzer, P., Lingemann,  
 1074 J., Magass, C., Merschmeyer, M., Meyer, A., Olschewski, M., Papacz, P., Pieta, H.,  
 1075 Reithler, H., Schmitz, S. A., Sonnenschein, L., Steggemann, J., Teyssier, D., Weber, M.,  
 1076 Bontenackels, M., Cherepanov, V., Flügge, G., Geenen, H., Geisler, M., Haj Ahmad, W.,  
 1077 Hoehle, F., Kargoll, B., Kress, T., Kuessel, Y., Nowack, A., Perchalla, L., Pooth, O.,  
 1078 Rennefeld, J., Sauerland, P., Stahl, A., Aldaya Martin, M., Behr, J., Behrenhoff, W.,  
 1079 Behrens, U., Bergholz, M., Bethani, A., Borrás, K., Burgmeier, A., Cakir, A., Calligaris,  
 1080 L., Campbell, A., Castro, E., Costanza, F., Dammann, D., Diez Pardos, C., Eckerlin, G.,  
 1081 Eckstein, D., Flucke, G., Geiser, A., Glushkov, I., Gunnellini, P., Habib, S., Hauk, J.,  
 1082 Jung, H., Kasemann, M., Katsas, P., Kleinwort, C., Kluge, H., Knutsson, A., Krämer, M.,  
 1083 Krücker, D., Kuznetsova, E., Lange, W., Lohmann, W., Lutz, B., Mankel, R., Marfin, I.,  
 1084 Marienfeld, M., Melzer-Pellmann, I.-A., Meyer, A. B., Mnich, J., Mussgiller, A., Naumann-  
 1085 Emme, S., Olzem, J., Perrey, H., Petrukhin, A., Pitzl, D., Raspereza, A., Ribeiro Cipriano,  
 1086 P. M., Riedl, C., Ron, E., Rosin, M., Salfeld-Nebgen, J., Schmidt, R., Schoerner-Sadenius,  
 1087 T., Sen, N., Spiridonov, A., Stein, M., Walsh, R., Wissing, C., Autermann, C., Blobel,  
 1088 V., Draeger, J., Enderle, H., Erfle, J., Gebbert, U., Görner, M., Hermanns, T., Höing,  
 1089 R. S., Kaschube, K., Kaussen, G., Kirschenmann, H., Klanner, R., Lange, J., Mura, B.,  
 1090 Nowak, F., Peiffer, T., Pietsch, N., Sander, C., Schettler, H., Schleper, P., Schlieckau, E.,

1091 Schmidt, A., Schröder, M., Schum, T., Sola, V., Stadie, H., Steinbrück, G., Thomsen,  
 1092 J., Vanelderden, L., Barth, C., Berger, J., Chwalek, T., De Boer, W., Dierlamm, A.,  
 1093 Feindt, M., Guthoff, M., Hackstein, C., Hartmann, F., Heinrich, M., Held, H., Hoffmann,  
 1094 K. H., Honc, S., Katkov, I., Komaragiri, J. R., Lobelle Pardo, P., Martschei, D., Mueller,  
 1095 S., Müller, T., Niegel, M., Nürnberg, A., Oberst, O., Oehler, A., Ott, J., Quast, G.,  
 1096 Rabbertz, K., Ratnikov, F., Ratnikova, N., Röcker, S., Scheurer, A., Schilling, F.-P.,  
 1097 Schott, G., Simonis, H. J., Stober, F. M., Troendle, D., Ulrich, R., Wagner-Kuhr, J.,  
 1098 Weiler, T., Zeise, M., Daskalakis, G., Geralis, T., Kesisoglou, S., Kyriakis, A., Loukas,  
 1099 D., Manolakos, I., Markou, A., Markou, C., Mavrommatis, C., Ntomari, E., Gouskos, L.,  
 1100 Mertzimekis, T. J., Panagiotou, A., Saoulidou, N., Evangelou, I., Foudas, C., Kokkas, P.,  
 1101 Manthos, N., Papadopoulos, I., Patras, V., Bencze, G., Hajdu, C., Hidas, P., Horvath, D.,  
 1102 Sikler, F., Veszpremi, V., Vesztergombi, G., Beni, N., Czellar, S., Molnar, J., Palinkas, J.,  
 1103 Szillasi, Z., Karancsi, J., Raics, P., Trocsanyi, Z. L., Ujvari, B., Beri, S. B., Bhatnagar,  
 1104 V., Dhingra, N., Gupta, R., Jindal, M., Kaur, M., Mehta, M. Z., Nishu, N., Saini, L. K.,  
 1105 Sharma, A., Singh, J., Ahuja, S., Bhardwaj, A., Choudhary, B. C., Kumar, A., Kumar,  
 1106 A., Malhotra, S., Naimuddin, M., Ranjan, K., Sharma, V., Shivpuri, R. K., Banerjee,  
 1107 S., Bhattacharya, S., Dutta, S., Gomber, B., Jain, S., Jain, S., Khurana, R., Sarkar,  
 1108 S., Sharan, M., Abdulsalam, A., Choudhury, R. K., Dutta, D., Kailas, S., Kumar, V.,  
 1109 Mehta, P., Mohanty, A. K., Pant, L. M., Shukla, P., Aziz, T., Ganguly, S., Guchait, M.,  
 1110 Maity, M., Majumder, G., Mazumdar, K., Mohanty, G. B., Parida, B., Sudhakar, K.,  
 1111 Wickramage, N., Banerjee, S., Dugad, S., Arfaei, H., Bakhshiansohi, H., Etesami, S. M.,  
 1112 Fahim, A., Hashemi, M., Hesari, H., Jafari, A., Khakzad, M., Mohammadi Najafabadi,  
 1113 M., Paktinat Mehdiabadi, S., Safarzadeh, B., Zeinali, M., Abbrescia, M., Barbone, L.,  
 1114 Calabria, C., Chhibra, S. S., Colaleo, A., Creanza, D., De Filippis, N., De Palma, M.,  
 1115 Fiore, L., Iaselli, G., Lusito, L., Maggi, G., Maggi, M., Marangelli, B., My, S., Nuzzo,  
 1116 S., Pacifico, N., Pompili, A., Pugliese, G., Selvaggi, G., Silvestris, L., Singh, G., Zito,  
 1117 G., Abbiendi, G., Benvenuti, A. C., Bonacorsi, D., Braibant-Giacomelli, S., Brigliadori,  
 1118 L., Capiluppi, P., Castro, A., Cavallo, F. R., Cuffiani, M., Dallavalle, G. M., Fabbri, F.,  
 1119 Fanfani, A., Fasanella, D., Giacomelli, P., Grandi, C., Guiducci, L., Marcellini, S., Masetti,  
 1120 G., Meneghelli, M., Montanari, A., Navarria, F. L., Odorici, F., Perrotta, A., Primavera,

1121 F., Rossi, A. M., Rovelli, T., Siroli, G., Travaglini, R., Albergo, S., Cappello, G., Chiorboli,  
 1122 M., Costa, S., Potenza, R., Tricomi, A., Tuve, C., Barbagli, G., Ciulli, V., Civinini, C.,  
 1123 D'Alessandro, R., Focardi, E., Frosali, S., Gallo, E., Gonzi, S., Meschini, M., Paoletti,  
 1124 S., Sguazzoni, G., Tropiano, A., Benussi, L., Bianco, S., Colafranceschi, S., Fabbri, F.,  
 1125 Piccolo, D., Fabbricatore, P., Musenich, R., Benaglia, A., De Guio, F., Di Matteo, L.,  
 1126 Fiorendi, S., Gennai, S., Ghezzi, A., Malvezzi, S., Manzoni, R. A., Martelli, A., Massironi,  
 1127 A., Menasce, D., Moroni, L., Paganoni, M., Pedrini, D., Ragazzi, S., Redaelli, N., Sala,  
 1128 S., Tabarelli de Fatis, T., Buontempo, S., Carrillo Montoya, C. A., Cavallo, N., De Cosa,  
 1129 A., Dogangun, O., Fabozzi, F., Iorio, A. O. M., Lista, L., Meola, S., Merola, M., Paolucci,  
 1130 P., Azzi, P., Bacchetta, N., Bellan, P., Bisello, D., Branca, A., Carlin, R., Checchia, P.,  
 1131 Dorigo, T., Dosselli, U., Gasparini, F., Gasparini, U., Gozzelino, A., Kanishchev, K.,  
 1132 Lacaprara, S., Lazzizzera, I., Margoni, M., Meneguzzo, A. T., Nespolo, M., Ronchese,  
 1133 P., Simonetto, F., Torassa, E., Vanini, S., Zotto, P., Zumerle, G., Gabusi, M., Ratti,  
 1134 S. P., Riccardi, C., Torre, P., Vitulo, P., Biasini, M., Bilei, G. M., Fanò, L., Lariccia, P.,  
 1135 Lucaroni, A., Mantovani, G., Menichelli, M., Nappi, A., Romeo, F., Saha, A., Santocchia,  
 1136 A., Taroni, S., Azzurri, P., Bagliesi, G., Boccali, T., Broccolo, G., Castaldi, R., D'Agnolo,  
 1137 R. T., Dell'Orso, R., Fiori, F., Foà, L., Giassi, A., Kraan, A., Ligabue, F., Lomtadze, T.,  
 1138 Martini, L., Messineo, A., Palla, F., Rizzi, A., Serban, A. T., Spagnolo, P., Squillacioti, P.,  
 1139 Tenchini, R., Tonelli, G., Venturi, A., Verdini, P. G., Barone, L., Cavallari, F., Del Re, D.,  
 1140 Diemoz, M., Grassi, M., Longo, E., Meridiani, P., Micheli, F., Nourbakhsh, S., Organtini,  
 1141 G., Paramatti, R., Rahatlou, S., Sigamani, M., Soffi, L., Amapane, N., Arcidiacono, R.,  
 1142 Argiro, S., Arneodo, M., Biino, C., Cartiglia, N., Costa, M., Demaria, N., Graziano,  
 1143 A., Mariotti, C., Maselli, S., Migliore, E., Monaco, V., Musich, M., Obertino, M. M.,  
 1144 Pastrone, N., Pelliccioni, M., Potenza, A., Romero, A., Ruspa, M., Sacchi, R., Solano, A.,  
 1145 Staiano, A., Vilela Pereira, A., Belforte, S., Candelise, V., Cossutti, F., Della Ricca, G.,  
 1146 Gobbo, B., Marone, M., Montanino, D., Penzo, A., Schizzi, A., Heo, S. G., Kim, T. Y.,  
 1147 Nam, S. K., Chang, S., Kim, D. H., Kim, G. N., Kong, D. J., Park, H., Ro, S. R., Son,  
 1148 D. C., Son, T., Kim, J. Y., Kim, Z. J., Song, S., Choi, S., Gyun, D., Hong, B., Jo, M.,  
 1149 Kim, H., Kim, T. J., Lee, K. S., Moon, D. H., Park, S. K., Choi, M., Kim, J. H., Park,  
 1150 C., Park, I. C., Park, S., Ryu, G., Cho, Y., Choi, Y., Choi, Y. K., Goh, J., Kim, M. S.,

1151 Kwon, E., Lee, B., Lee, J., Lee, S., Seo, H., Yu, I., Bilinskas, M. J., Grigelionis, I., Janulis,  
 1152 M., Juodagalvis, A., Castilla-Valdez, H., De La Cruz-Burelo, E., Heredia-de La Cruz, I.,  
 1153 Lopez-Fernandez, R., Magaña Villalba, R., Martínez-Ortega, J., Sánchez-Hernández, A.,  
 1154 Villasenor-Cendejas, L. M., Carrillo Moreno, S., Vazquez Valencia, F., Salazar Ibarguen,  
 1155 H. A., Casimiro Linares, E., Morelos Pineda, A., Reyes-Santos, M. A., Krofcheck, D.,  
 1156 Bell, A. J., Butler, P. H., Doesburg, R., Reucroft, S., Silverwood, H., Ahmad, M.,  
 1157 Asghar, M. I., Hoorani, H. R., Khalid, S., Khan, W. A., Khurshid, T., Qazi, S., Shah,  
 1158 M. A., Shoaib, M., Bialkowska, H., Boimska, B., Frueboes, T., Gokieli, R., Górski,  
 1159 M., Kazana, M., Nawrocki, K., Romanowska-Rybinska, K., Szleper, M., Wrochna, G.,  
 1160 Zalewski, P., Brona, G., Bunkowski, K., Cwiok, M., Dominik, W., Doroba, K., Kalinowski,  
 1161 A., Konecki, M., Krolkowski, J., Almeida, N., Bargassa, P., David, A., Faccioli, P.,  
 1162 Ferreira Parracho, P. G., Gallinaro, M., Seixas, J., Varela, J., Vischia, P., Belotelov,  
 1163 I., Bunin, P., Gavrilenko, M., Golutvin, I., Gorbunov, I., Kamenev, A., Karjavin, V.,  
 1164 Kozlov, G., Lanev, A., Malakhov, A., Moisenz, P., Palichik, V., Pereygin, V., Shmatov,  
 1165 S., Smirnov, V., Volodko, A., Zarubin, A., Evstyukhin, S., Golovtsov, V., Ivanov, Y.,  
 1166 Kim, V., Levchenko, P., Murzin, V., Oreshkin, V., Smirnov, I., Sulimov, V., Uvarov,  
 1167 L., Vavilov, S., Vorobyev, A., Vorobyev, A., Andreev, Y., Dermenev, A., Gninenko,  
 1168 S., Golubev, N., Kirsanov, M., Krasnikov, N., Matveev, V., Pashenkov, A., Tlisov, D.,  
 1169 Toropin, A., Epshteyn, V., Erofeeva, M., Gavrilov, V., Kossov, M., Lychkovskaya, N.,  
 1170 Popov, V., Safronov, G., Semenov, S., Stolin, V., Vlasov, E., Zhokin, A., Belyaev, A.,  
 1171 Boos, E., Ershov, A., Gribushin, A., Klyukhin, V., Kodolova, O., Korotkikh, V., Lokhtin,  
 1172 I., Markina, A., Obraztsov, S., Perfilov, M., Petrushanko, S., Popov, A., Sarycheva, L.,  
 1173 Savrin, V., Snigirev, A., Vardanyan, I., Andreev, V., Azarkin, M., Dremin, I., Kirakosyan,  
 1174 M., Leonidov, A., Mesyats, G., Rusakov, S. V., Vinogradov, A., Azhgirey, I., Bayshev, I.,  
 1175 Bitioukov, S., Grishin, V., Kachanov, V., Konstantinov, D., Korablev, A., Krychkine,  
 1176 V., Petrov, V., Ryutin, R., Sobol, A., Tourtchanovitch, L., Troshin, S., Tyurin, N.,  
 1177 Uzunian, A., Volkov, A., Adzic, P., Djordjevic, M., Ekmedzic, M., Krpic, D., Milosevic, J.,  
 1178 Aguilar-Benitez, M., Alcaraz Maestre, J., Arce, P., Battilana, C., Calvo, E., Cerrada, M.,  
 1179 Chamizo Llatas, M., Colino, N., De La Cruz, B., Delgado Peris, A., Domínguez Vázquez,  
 1180 D., Fernandez Bedoya, C., Fernández Ramos, J. P., Ferrando, A., Flix, J., Fouz, M. C.,

1181 Garcia-Abia, P., Gonzalez Lopez, O., Goy Lopez, S., Hernandez, J. M., Josa, M. I., Merino,  
 1182 G., Puerta Pelayo, J., Quintario Olmeda, A., Redondo, I., Romero, L., Santaolalla, J.,  
 1183 Soares, M. S., Willmott, C., Albajar, C., Codispoti, G., de Trocóniz, J. F., Brun, H.,  
 1184 Cuevas, J., Fernandez Menendez, J., Folgueras, S., Gonzalez Caballero, I., Lloret Iglesias,  
 1185 L., Piedra Gomez, J., Brochero Cifuentes, J. A., Cabrillo, I. J., Calderon, A., Chuang,  
 1186 S. H., Duarte Campderros, J., Felcini, M., Fernandez, M., Gomez, G., Gonzalez Sanchez,  
 1187 J., Jorda, C., Lopez Virto, A., Marco, J., Marco, R., Martinez Rivero, C., Matorras,  
 1188 F., Munoz Sanchez, F. J., Rodrigo, T., Rodríguez-Marrero, A. Y., Ruiz-Jimeno, A.,  
 1189 Scodellaro, L., Sobron Sanudo, M., Vila, I., Vilar Cortabitarte, R., Abbaneo, D., Auffray,  
 1190 E., Auzinger, G., Baillon, P., Ball, A. H., Barney, D., Benitez, J. F., Bernet, C., Bianchi,  
 1191 G., Bloch, P., Bocci, A., Bonato, A., Botta, C., Breuker, H., Camporesi, T., Cerminara,  
 1192 G., Christiansen, T., Coarasa Perez, J. A., D'Enterria, D., Dabrowski, A., De Roeck,  
 1193 A., Di Guida, S., Dobson, M., Dupont-Sagorin, N., Elliott-Peisert, A., Frisch, B., Funk,  
 1194 W., Georgiou, G., Giffels, M., Gigi, D., Gill, K., Giordano, D., Giunta, M., Glege, F.,  
 1195 Gomez-Reino Garrido, R., Govoni, P., Gowdy, S., Guida, R., Hansen, M., Harris, P.,  
 1196 Hartl, C., Harvey, J., Hegner, B., Hinzmann, A., Innocente, V., Janot, P., Kaadze, K.,  
 1197 Karavakis, E., Kousouris, K., Lecoq, P., Lee, Y.-J., Lenzi, P., Lourenço, C., Mäki, T.,  
 1198 Malberti, M., Malgeri, L., Mannelli, M., Masetti, L., Meijers, F., Mersi, S., Meschi, E.,  
 1199 Moser, R., Mozer, M. U., Mulders, M., Musella, P., Nesvold, E., Orimoto, T., Orsini, L.,  
 1200 Palencia Cortezon, E., Perez, E., Perrozzi, L., Petrilli, A., Pfeiffer, A., Pierini, M., Pimiä,  
 1201 M., Piparo, D., Polese, G., Quertenmont, L., Racz, A., Reece, W., Rodrigues Antunes, J.,  
 1202 Rolandi, G., Rommerskirchen, T., Rovelli, C., Rovere, M., Sakulin, H., Santanastasio, F.,  
 1203 Schäfer, C., Schwick, C., Segoni, I., Sekmen, S., Sharma, A., Siegrist, P., Silva, P., Simon,  
 1204 M., Sphicas, P., Spiga, D., Spiropulu, M., Tsirou, A., Veres, G. I., Vlimant, J. R., Wöhri,  
 1205 H. K., Worm, S. D., Zeuner, W. D., Bertl, W., Deiters, K., Erdmann, W., Gabathuler,  
 1206 K., Horisberger, R., Ingram, Q., Kaestli, H. C., König, S., Kotlinski, D., Langenegger, U.,  
 1207 Meier, F., Renker, D., Rohe, T., Sibille, J., Bäni, L., Bortignon, P., Buchmann, M. A.,  
 1208 Casal, B., Chanon, N., Deisher, A., Dissertori, G., Dittmar, M., Dünser, M., Eugster, J.,  
 1209 Freudenreich, K., Grab, C., Hits, D., Lecomte, P., Lustermann, W., Martinez Ruiz del  
 1210 Arbol, P., Mohr, N., Moortgat, F., Nägeli, C., Nef, P., Nessi-Tedaldi, F., Pandolfi, F.,

1211 Pape, L., Pauss, F., Peruzzi, M., Ronga, F. J., Rossini, M., Sala, L., Sanchez, A. K.,  
 1212 Starodumov, A., Stieger, B., Takahashi, M., Tauscher, L., Thea, A., Theofilatos, K.,  
 1213 Treille, D., Urscheler, C., Wallny, R., Weber, H. A., Wehrli, L., Aguilo, E., Amsler, C.,  
 1214 Chiochia, V., De Visscher, S., Favaro, C., Ivova Rikova, M., Millan Mejias, B., Otiougova,  
 1215 P., Robmann, P., Snoek, H., Tupputi, S., Verzetti, M., Chang, Y. H., Chen, K. H., Kuo,  
 1216 C. M., Li, S. W., Lin, W., Liu, Z. K., Lu, Y. J., Mekterovic, D., Singh, A. P., Volpe, R., Yu,  
 1217 S. S., Bartalini, P., Chang, P., Chang, Y. H., Chang, Y. W., Chao, Y., Chen, K. F., Dietz,  
 1218 C., Grundler, U., Hou, W.-S., Hsiung, Y., Kao, K. Y., Lei, Y. J., Lu, R.-S., Majumder, D.,  
 1219 Petrakou, E., Shi, X., Shiu, J. G., Tzeng, Y. M., Wan, X., Wang, M., Adiguzel, A., Bakirci,  
 1220 M. N., Cerci, S., Dozen, C., Dumanoglu, I., Eskut, E., Girgis, S., Gokbulut, G., Gurpinar,  
 1221 E., Hos, I., Kangal, E. E., Karapinar, G., Kayis Topaksu, A., Onengut, G., Ozdemir, K.,  
 1222 Ozturk, S., Polatoz, A., Sogut, K., Sunar Cerci, D., Tali, B., Topakli, H., Vergili, L. N.,  
 1223 Vergili, M., Akin, I. V., Aliev, T., Bilin, B., Bilmis, S., Deniz, M., Gamsizkan, H., Guler,  
 1224 A. M., Ocalan, K., Ozpineci, A., Serin, M., Sever, R., Surat, U. E., Yalvac, M., Yildirim,  
 1225 E., Zeyrek, M., Gülmez, E., Isildak, B., Kaya, M., Kaya, O., Ozkorucuklu, S., Sonmez, N.,  
 1226 Cankocak, K., Levchuk, L., Bostock, F., Brooke, J. J., Clement, E., Cussans, D., Flacher,  
 1227 H., Frazier, R., Goldstein, J., Grimes, M., Heath, G. P., Heath, H. F., Kreczko, L.,  
 1228 Metson, S., Newbold, D. M., Nirunpong, K., Poll, A., Senkin, S., Smith, V. J., Williams,  
 1229 T., Basso, L., Bell, K. W., Belyaev, A., Brew, C., Brown, R. M., Cockerill, D. J. A.,  
 1230 Coughlan, J. A., Harder, K., Harper, S., Jackson, J., Kennedy, B. W., Olaiya, E., Petyt,  
 1231 D., Radburn-Smith, B. C., Shepherd-Themistocleous, C. H., Tomalin, I. R., Womersley,  
 1232 W. J., Bainbridge, R., Ball, G., Beuselinck, R., Buchmuller, O., Colling, D., Cripps, N.,  
 1233 Cutajar, M., Dauncey, P., Davies, G., Della Negra, M., Ferguson, W., Fulcher, J., Futyan,  
 1234 D., Gilbert, A., Guneratne Bryer, A., Hall, G., Hatherell, Z., Hays, J., Iles, G., Jarvis,  
 1235 M., Karapostoli, G., Lyons, L., Magnan, A.-M., Marrouche, J., Mathias, B., Nandi, R.,  
 1236 Nash, J., Nikitenko, A., Papageorgiou, A., Pela, J., Pesaresi, M., Petridis, K., Pioppi,  
 1237 M., Raymond, D. M., Rogerson, S., Rose, A., Ryan, M. J., Seez, C., Sharp, P., Sparrow,  
 1238 A., Stoye, M., Tapper, A., Vazquez Acosta, M., Virdee, T., Wakefield, S., Wardle, N.,  
 1239 Whyntie, T., Chadwick, M., Cole, J. E., Hobson, P. R., Khan, A., Kyberd, P., Leslie, D.,  
 1240 Martin, W., Reid, I. D., Symonds, P., Teodorescu, L., Turner, M., Hatakeyama, K., Liu,

H., Scarborough, T., Charaf, O., Henderson, C., Rumerio, P., Avetisyan, A., Bose, T.,  
Fantasia, C., Heiste (2012). Measurement of the pseudorapidity and centrality dependence  
of the transverse energy density in pb-pb collisions at  $\sqrt{s_{\text{NN}}} = 2.76$  TeV. *Phys. Rev. Lett.*,  
109:152303. 6, 22

[12] Collaboration, T. A., Aamodt, K., Quintana, A. A., Achenbach, R., Acounis, S.,  
Adamov, D., Adler, C., Aggarwal, M., Agnese, F., Rinella, G. A., Ahammed, Z., Ahmad,  
A., Ahmad, N., Ahmad, S., Akindinov, A., Akishin, P., Aleksandrov, D., Alessandro,  
B., Alfaro, R., Alfarone, G., Alici, A., Alme, J., Alt, T., Altinpinar, S., Amend, W.,  
Andrei, C., Andres, Y., Andronic, A., Anelli, G., Anfreville, M., Angelov, V., Anzo, A.,  
Anson, C., Antici, T., Antonenko, V., Antonczyk, D., Antinori, F., Antinori, S., Antonioli,  
P., Aphecetche, L., Appelshuser, H., Aprodu, V., Arba, M., Arcelli, S., Argentieri, A.,  
Armesto, N., Arnaldi, R., Arefiev, A., Arsene, I., Asryan, A., Augustinus, A., Awes, T. C.,  
ysto, J., Azmi, M. D., Bablock, S., Badal, A., Badyal, S. K., Baechler, J., Bagnasco, S.,  
Bailhache, R., Bala, R., Baldisseri, A., Baldit, A., Bn, J., Barbera, R., Barberis, P.-L.,  
Barbet, J. M., Barnfoldi, G., Barret, V., Bartke, J., Bartos, D., Basile, M., Basmanov, V.,  
Bastid, N., Batigne, G., Batyunya, B., Baudot, J., Baumann, C., Bearden, I., Becker, B.,  
Belikov, J., Bellwied, R., Belmont-Moreno, E., Belogianni, A., Belyaev, S., Benato, A.,  
Beney, J. L., Benhabib, L., Benotto, F., Beol, S., Berceanu, I., Bercuci, A., Berdermann,  
E., Berdnikov, Y., Bernard, C., Berny, R., Berst, J. D., Bertelsen, H., Betev, L., Bhasin,  
A., Baskar, P., Bhati, A., Bianchi, N., Bielik, J., Bielikov, J., Bimbot, L., Blanchard, G.,  
Blanco, F., Blanco, F., Blau, D., Blume, C., Blyth, S., Boccioni, M., Bogdanov, A., Bggild,  
H., Bogolyubsky, M., Boldizsr, L., Bombara, M., Bombonati, C., Bondila, M., Bonnet,  
D., Bonvicini, V., Borel, H., Borotto, F., Borshchov, V., Bortoli, Y., Borysov, O., Bose,  
S., Bosisio, L., Botje, M., Bttger, S., Bourdaud, G., Bourrion, O., Bouvier, S., Braem,  
A., Braun, M., Braun-Munzinger, P., Bravina, L., Bregant, M., Bruckner, G., Brun, R.,  
Bruna, E., Brunasso, O., Bruno, G. E., Bucher, D., Budilov, V., Budnikov, D., Buesching,  
H., Buncic, P., Burns, M., Burachas, S., Busch, O., Bushop, J., Cai, X., Caines, H.,  
Calaon, F., Caldogno, M., Cali, I., Camerini, P., Campagnolo, R., Campbell, M., Cao,  
X., Capitani, G. P., Romeo, G. C., Cardenas-Montes, M., Carduner, H., Carena, F.,

1270 Carena, W., Cariola, P., Carminati, F., Casado, J., Diaz, A. C., Caselle, M., Castellanos,  
 1271 J. C., Castor, J., Catanescu, V., Cattaruzza, E., Cavazza, D., Cerello, P., Ceresa, S.,  
 1272 ern, V., Chambert, V., Chapeland, S., Charpy, A., Charrier, D., Chartoire, M., Charvet,  
 1273 J. L., Chattopadhyay, S., Chattopadhyay, S., Chepurnov, V., Chernenko, S., Cherney,  
 1274 M., Cheshkov, C., Cheynis, B., Chochula, P., Chiavassa, E., Barroso, V. C., Choi, J.,  
 1275 Christakoglou, P., Christiansen, P., Christensen, C., Chykalov, O. A., Cicalo, C., Cifarelli-  
 1276 Strolin, L., Ciobanu, M., Cindolo, F., Cirstoiu, C., Clausse, O., Cleymans, J., Cobanoglu,  
 1277 O., Coffin, J.-P., Coli, S., Colla, A., Colledani, C., Combaret, C., Combet, M., Comets,  
 1278 M., Balbastre, G. C., del Valle, Z. C., Contin, G., Contreras, J., Cormier, T., Corsi, F.,  
 1279 Cortese, P., Costa, F., Crescio, E., Crochet, P., Cuautle, E., Cussonneau, J., Dahlinger,  
 1280 M., Dainese, A., Dalsgaard, H. H., Daniel, L., Das, I., Das, T., Dash, A., Silva, R. D.,  
 1281 Davenport, M., Daues, H., Caro, A. D., de Cataldo, G., Cuveland, J. D., Falco, A. D.,  
 1282 de Gaspari, M., de Girolamo, P., de Groot, J., Gruttola, D. D., Haas, A. D., Marco, N. D.,  
 1283 Pasquale, S. D., Remigis, P. D., de Vaux, D., Decock, G., Delagrange, H., Franco, M. D.,  
 1284 Dellacasa, G., Dell'Olio, C., Dell'Olio, D., Deloff, A., Demanov, V., Dnes, E., D'Erasmus,  
 1285 G., Derkach, D., Devaux, A., Bari, D. D., Bartolomeo, A. D., Giglio, C. D., Liberto,  
 1286 S. D., Mauro, A. D., Nezza, P. D., Dialinas, M., Diaz, L., Valdes, R. D., Dietel, T., Dima,  
 1287 R., Ding, H., Dinca, C., Divi, R., Dobretsov, V., Dobrin, A., Doenigus, B., Dobrowolski,  
 1288 T., Domnguez, I., Dorn, M., Drouet, S., Dubey, A. E., Ducroux, L., Dumitrache, F.,  
 1289 Dumonteil, E., Dupieux, P., Duta, V., Majumdar, A. D., Majumdar, M. D., Dyhre,  
 1290 T., Efimov, L., Efremov, A., Elia, D., Emschermann, D., Engster, C., Enokizono, A.,  
 1291 Espagnon, B., Estienne, M., Evangelista, A., Evans, D., Evrard, S., Fabjan, C. W.,  
 1292 Fabris, D., Faivre, J., Falchieri, D., Fantoni, A., Farano, R., Fearick, R., Fedorov, O.,  
 1293 Fekete, V., Felea, D., Feofilov, G., Tllez, A. F., Ferretti, A., Fichera, F., Filchagin, S.,  
 1294 Filoni, E., Finck, C., Fini, R., Fiore, E. M., Flierl, D., Floris, M., Fodor, Z., Foka, Y.,  
 1295 Fokin, S., Force, P., Formenti, F., Fragiaco, E., Fragiadakis, M., Fraissard, D., Franco,  
 1296 A., Franco, M., Frankenfeld, U., Fratino, U., Fresneau, S., Frolov, A., Fuchs, U., Fujita, J.,  
 1297 Furget, C., Furini, M., Girard, M. F., Gaardhje, J.-J., Gabrielli, A., Gadrat, S., Gagliardi,  
 1298 M., Gago, A., Gaido, L., Torreira, A. G., Gallio, M., Gandolfi, E., Ganoti, P., Ganti, M.,  
 1299 Garabatos, J., Lopez, A. G., Garizzo, L., Gaudichet, L., Gemme, R., Germain, M., Gheata,



1300 A., Gheata, M., Ghidini, B., Ghosh, P., Giolu, G., Giraudo, G., Giubellino, P., Glasow,  
 1301 R., Glssel, P., Ferreira, E. G., Gutierrez, C. G., Gonzales-Trueba, L. H., Gorbunov, S.,  
 1302 Gorbunov, Y., Gos, H., Gosset, J., Gotovac, S., Gottschlag, H., Gottschalk, D., Grabski,  
 1303 V., Grassi, T., Gray, H., Grebenyuk, O., Grebieszko, K., Gregory, C., Grigoras, C.,  
 1304 Grion, N., Grigoriev, V., Grigoryan, A., Grigoryan, C., Grigoryan, S., Grishuk, Y., Gros,  
 1305 P., Grosse-Oetringhaus, J., Grossiord, J.-Y., Grosso, R., Grynyov, B., Guarnaccia, C.,  
 1306 Guber, F., Guerin, F., Guernane, R., Guerzoni, M., Guichard, A., Guida, M., Guilloux,  
 1307 G., Gulkanyan, H., Gulbrandsen, K., Gunji, T., Gupta, A., Gupta, V., Gustafsson, H.-  
 1308 A., Gutbrod, H., Hadjidakis, C., Haiduc, M., Hamar, G., Hamagaki, H., Hamblen, J.,  
 1309 Hansen, J. C., Hardy, P., Hatzifotiadou, D., Harris, J. W., Hartig, M., Harutyunyan, A.,  
 1310 Hayrapetyan, A., Hasch, D., Hasegan, D., Hehner, J., Heine, N., Heinz, M., Helstrup, H.,  
 1311 Herghelegiu, A., Herlant, S., Corral, G. H., Herrmann, N., Hetland, K., Hille, P., Hinke,  
 1312 H., Hippolyte, B., Hoch, M., Hoebbel, H., Hoedlmoser, H., Horaguchi, T., Horner, M.,  
 1313 Hristov, P., Hrivnov, I., Hu, S., Guo, C. H., Humanic, T., Hurtado, A., Hwang, D. S.,  
 1314 Ianigro, J. C., Idzik, M., Igoikin, S., Ilkaev, R., Ilkiv, I., Imhoff, M., Innocenti, P. G.,  
 1315 Ionescu, E., Ippolitov, M., Irfan, M., Insa, C., Inuzuka, M., Ivan, C., Ivanov, A., Ivanov,  
 1316 M., Ivanov, V., Jacobs, P., Jacholkowski, A., Janurov, L., Janik, R., Jasper, M., Jena, C.,  
 1317 Jirde, L., Johnson, D. P., Jones, G. T., Jorgensen, C., Jouve, F., Jovanovi, P., Junique,  
 1318 A., Jusko, A., Jung, H., Jung, W., Kadija, K., Kamal, A., Kamermans, R., Kapusta, S.,  
 1319 Kaidalov, A., Kakoyan, V., Kalcher, S., Kang, E., Kapitan, J., Kaplin, V., Karadzhev, K.,  
 1320 Karavichev, O., Karavicheva, T., Karpechev, E., Karpio, K., Kazantsev, A., Kebschull,  
 1321 U., Keidel, R., Khan, M. M., Khanzadeev, A., Kharlov, Y., Kikola, D., Kileng, B., Kim,  
 1322 D., Kim, D. S., Kim, D. W., Kim, H. N., Kim, J. S., Kim, S., Kinson, J. B., Kiprich, S. K.,  
 1323 Kisel, I., Kiselev, S., Kisiel, A., Kiss, T., Kiworra, V., Klay, J., Bsing, C. K., Kliemant, M.,  
 1324 Klimov, A., Klovning, A., Kluge, A., Kluit, R., Kniege, S., Kolevatov, R., Kollegger, T.,  
 1325 Kolojvari, A., Kondratiev, V., Kornas, E., Koshurnikov, E., Kotov, I., Kour, R., Kowalski,  
 1326 M., Kox, S., Kozlov, K., Krlik, I., Kramer, F., Kraus, I., Kravkov, A., Krawutschke, T.,  
 1327 Krivda, M., Kryshen, E., Kucheriaev, Y., Kugler, A., Kuhn, C., Kuijer, P., Kumar, L.,  
 1328 Kumar, N., Kumpumaeki, P., Kurepin, A., Kurepin, A. N., Kushpil, S., Kushpil, V.,  
 1329 Kutovsky, M., Kvaerno, H., Kweon, M., Labb, J.-C., Lackner, F., de Guevara, P. L.,

1330 Lafage, V., Rocca, P. L., Lamont, M., Lara, C., Larsen, D. T., Laurenti, G., Lazzeroni,  
 1331 C., Bornec, Y. L., Bris, N. L., Gailliard, C. L., Lebedev, V., Lecoq, J., Lee, K. S., Lee, S. C.,  
 1332 Lefvre, F., Legrand, I., Lehmann, T., Leistam, L., Lenoir, P., Lenti, V., Leon, H., Monzon,  
 1333 I. L., Lvai, P., Li, Q., Li, X., Librizzi, F., Lietava, R., Lindegaard, N., Lindenstruth, V.,  
 1334 Lippmann, C., Lisa, M., Listratenko, O. M., Littel, F., Liu, Y., Lo, J., Lobanov, V.,  
 1335 Loginov, V., Noriega, M. L., Lpez-Ramrez, R., Torres, E. L., Lorenzo, P. M., Lvhidden,  
 1336 G., Lu, S., Ludolphs, W., Lunardon, M., Luquin, L., Lusso, S., Lutz, J.-R., Luvisetto,  
 1337 M., Lyapin, V., Maevskaya, A., Magureanu, C., Mahajan, A., Majahan, S., Mahmoud,  
 1338 T., Mairani, A., Mahapatra, D., Makarov, A., Makhlyueva, I., Malek, M., Malkiewicz,  
 1339 T., Mal'Kevich, D., Malzacher, P., Mamonov, A., Manea, C., Mangotra, L. K., Maniero,  
 1340 D., Manko, V., Manso, F., Manzari, V., Mao, Y., Marcel, A., Marchini, S., Mare, J.,  
 1341 Margagliotti, G. V., Margotti, A., Marin, A., Marin, J.-C., Marras, D., Martinengo, P.,  
 1342 Martnez, M. I., Martinez-Davalos, A., Garcia, G. M., Martini, S., Chiesa, A. M., Marzocca,  
 1343 C., Masciocchi, S., Masera, M., Masetti, M., Maslov, N. I., Masoni, A., Massera, F., Mast,  
 1344 M., Mastroserio, A., Matthews, Z. L., Mayer, B., Mazza, G., Mazzaro, M. D., Mazzoni,  
 1345 A., Meddi, F., Meleshko, E., Menchaca-Rocha, A., Meneghini, S., Meoni, M., Perez, J. M.,  
 1346 Mereu, P., Meunier, O., Miake, Y., Michalon, A., Michinelli, R., Miftakhov, N., Mignone,  
 1347 M., Mikhailov, K., Milosevic, J., Minaev, Y., Minafra, F., Mischke, A., Mikowiec, D.,  
 1348 Mitsyn, V., Mitu, C., Mohanty, B., Moisa, D., Molnar, L., Mondal, M., Mondal, N.,  
 1349 Zetina, L. M., Monteno, M., Morando, M., Morel, M., Moretto, S., Morhardt, T., Morsch,  
 1350 A., Moukhanova, T., Mucchi, M., Muccifora, V., Mudnic, E., Mller, H., Mller, W., Munoz,  
 1351 J., Mura, D., Musa, L., Muraz, J. F., Musso, A., Nania, R., Nandi, B., Nappi, E., Navach,  
 1352 F., Navin, S., Nayak, T., Nazarenko, S., Nazarov, G., Nellen, L., Nendaz, F., Nianine,  
 1353 A., Nicassio, M., Nielsen, B. S., Nikolaev, S., Nikolic, V., Nikulin, S., Nikulin, V., Nilsen,  
 1354 B., Nitti, M., Noferini, F., Nomokonov, P., Nooren, G., Noto, F., Nouais, D., Nyiri,  
 1355 A., Nystrand, J., Odyniec, G., Oeschler, H., Oinonen, M., Oldenburg, M., Oleks, I.,  
 1356 Olsen, E. K., Onuchin, V., Oppedisano, C., Orsini, F., Ortiz-Velzquez, A., Oskamp, C.,  
 1357 Oskarsson, A., Osmic, F., sterman, L., Otterlund, I., Ovrebekk, G., Oyama, K., Pachr,  
 1358 M., Pagano, P., Pai, G., Pajares, C., Pal, S., Pal, S., Plla, G., Palmeri, A., Pancaldi,  
 1359 G., Panse, R., Pantaleo, A., Pappalardo, G. S., Pastirk, B., Pastore, C., Patarakin, O.,

1360 Paticchio, V., Patimo, G., Pavlinov, A., Pawlak, T., Peitzmann, T., Pnichot, Y., Pepato,  
 1361 A., Pereira, H., Peresunko, D., Perez, C., Griffo, J. P., Perini, D., Perrino, D., Peryt, W.,  
 1362 Pesci, A., Peskov, V., Pestov, Y., Peters, A. J., Petrek, V., Petridis, A., Petris, M., Petrov,  
 1363 V., Petrov, V., Petrovici, M., Peyr, J., Piano, S., Piccotti, A., Pichot, P., Piemonte, C.,  
 1364 Pikna, M., Pilastrini, R., Pillot, P., Pinazza, O., Pini, B., Pinsky, L., Morais, V. P.,  
 1365 Pismennaya, V., Piuz, F., Platt, R., Ploskon, M., Plumeri, S., Pluta, J., Pocheptsov,  
 1366 T., Podesta, P., Poggio, F., Poghosyan, M., Poghosyan, T., Polk, K., Polichtchouk, B.,  
 1367 Polozov, P., Polyakov, V., Pommeresch, B., Pompei, F., Pop, A., Popescu, S., Posa, F.,  
 1368 Pospil, V., Potukuchi, B., Pouthas, J., Prasad, S., Preghenella, R., Prino, F., Prodan, L.,  
 1369 Prono, G., Protsenko, M. A., Pruneau, C. A., Przybyla, A., Pshenichnov, I., Puddu, G.,  
 1370 Pujahari, P., Pulvirenti, A., Punin, A., Punin, V., Putschke, J., Quartieri, J., Quercigh,  
 1371 E., Rachevskaya, I., Rachevski, A., Rademakers, A., Radomski, S., Radu, A., Rak, J.,  
 1372 Ramello, L., Raniwala, R., Raniwala, S., Rasmussen, O. B., Rasson, J., Razin, V., Read,  
 1373 K., Real, J., Redlich, K., Reichling, C., Renard, C., Renault, G., Renfordt, R., Reolon,  
 1374 A. R., Reshetin, A., Revol, J.-P., Reygers, K., Ricaud, H., Riccati, L., Ricci, R. A., Richter,  
 1375 M., Riedler, P., Rigalleau, L. M., Riggi, F., Riegler, W., Rindel, E., Riso, J., Rivetti, A.,  
 1376 Rizzi, M., Rizzi, V., Cahuantzi, M. R., Red, K., Rhricht, D., Romn-Lpez, S., Romanato, M.,  
 1377 Romita, R., Ronchetti, F., Rosinsky, P., Rosnet, P., Rossegger, S., Rossi, A., Rostchin,  
 1378 V., Rotondo, F., Roukoutakis, F., Rousseau, S., Roy, C., Roy, D., Roy, P., Royer, L.,  
 1379 Rubin, G., Rubio, A., Rui, R., Rusanov, I., Russo, G., Ruuskanen, V., Ryabinkin, E.,  
 1380 Rybicki, A., Sadovsky, S., afak, K., Sahoo, R., Saini, J., Saiz, P., Salur, S., Sambyal,  
 1381 S., Samsonov, V., ndor, L., Sandoval, A., Sann, H., Santiard, J.-C., Santo, R., Santoro,  
 1382 R., Sargsyan, G., Saturnini, P., Scapparone, E., Scarlassara, F., Schackert, B., Schiaua,  
 1383 C., Schicker, R., Schioler, T., Schippers, J. D., Schmidt, C., Schmidt, H., Schneider, R.,  
 1384 Schossmaier, K., Schukraft, J., Schutz, Y., Schwarz, K., Schweda, K., Schyns, E., Scioli,  
 1385 G., Scomparin, E., Snow, H., Sedykh, S., Segato, G., Sellitto, S., Semeria, F., Senyukov,  
 1386 S., Seppnen, H., Serici, S., Serkin, L., Serra, S., Sesselmann, T., Sevcenco, A., Sgura, I.,  
 1387 Shabratova, G., Shahoyan, R., Sharkov, E., Sharma, S., Shigaki, K., Shileev, K., Shukla,  
 1388 P., Shurygin, A., Shurygina, M., Sibiriak, Y., Siddi, E., Siemiarczuk, T., Sigward, M. H.,  
 1389 Silenzi, A., Silvermyr, D., Silvestri, R., Simili, E., Simion, V., Simon, R., Simonetti, L.,

Singaraju, R., Singhal, V., Sinha, B., Sinha, T., Siska, M., Sitz, B., Sitta, M., Skaali,  
 B., Skowronski, P., Slodkowski, M., Smirnov, N., Smykov, L., Snellings, R., Snoeys, W.,  
 Soegaard, C., Soerensen, J., Sokolov, O., Soldatov, A., Soloviev, A., Soltveit, H., Soltz,  
 R., Sommer, W., Soos, C., Soramel, F., Sorensen, S., Soyk, D., Spyropoulou-Stassinaki,  
 M., Stachel, J., Staley, F., Stan, I., Stavinskiy, A., Steckert, J., Stefanini, G., Stefanek,  
 G., Steinbeck, T., Stelzer, H., Stenlund, E., Stocco, D., Stockmeier, M., Stoicea, G.,  
 Stolpovsky, P., Strme, P., Stutzmann, J. S., Su, G., Sugitate, T., umbera, M., Suire, C.,  
 Susa, T., Kumar, K. S., Swoboda, D., Symons, J., Szarka, I., Szostak, A., Szuba, M.,  
 Szymanski, P., Tadel, M., Tagridis, C., Tan, L., Takaki, D. T., Taureg, H., Tauro, A.,  
 Tavlet, M., Munoz, G. T., Thder, J., Tieulent, R., Timmer, P., Tolyhy, T., Topilskaya,  
 N., de Matos, C. T., Torii, H., Toscano, L., Tosello, F., Tournaire, A., Traczyk, T., Trger,  
 G., Tromeur, W., Truesdale, D., Trzaska, W., Tsiledakis, G., Tsilis, E., Tsvetkov, A.,  
 Turcato, M., Turrise, R., Tuveri, M., Tveter, T., Tydesjo, H., Tykarski, L., Tywoniuk, K.,  
 Ugolini, E., Ullaland, K., Urbn, J., Urciuoli, G. M., Usai, G. L., Usseglio, M., Vacchi, A.,  
 Vala, M., Valiev, F., Vyvre, P. V., Brink, A. V. D., Eijndhoven, N. V., Kolk, N. V. D.,  
 van Leeuwen, M., Vannucci, L., Vanzetto, S., Vanuxem, J.-P., Vargas, M. A., Varma,  
 R., Vascotto, A., Vasiliev, A., Vassiliou, M., Vasta, P., Vechernin, V., Venaruzzo, M.,  
 Vercellin, E., Vergara, S., Verhoeven, W., Veronese, F., Vetlitskiy, I., Vernet, R., Victorov,  
 V., Vidak, L., Viesti, G., Vikhlyantsev, O., Vilakazi, Z., Baillie, O. V., Vinogradov, A.,  
 Vinogradov, L., Vinogradov, Y., Virgili, T., Viyogi, Y., Vodopianov, A., Volpe, G., Vranic,  
 D., Vrlkov, J., Vulpescu, B., Wabnitz, C., Wagner, V., Wallet, L., Wan, R., Wang, Y.,  
 Wang, Y., Wheadon, R., Weis, R., Wen, Q., Wessels, J., Westergaard, J., Wiechula, J.,  
 Wiesenaecker, A., Wikne, J., Wilk, A., Wilk, G., Williams, C., Willis, N., Windelband, B.,  
 Witt, R., Woehri, H., Wyllie, K., Xu, C., Yang, C., Yang, H., Yermia, F., Yin, Z., Yin, Z.,  
 Ky, B. Y., Yushmanov, I., Yuting, B., Zabrodin, E., Zagato, S., Zagreev, B., Zaharia, P.,  
 Zalite, A., Zampa, G., Zampolli, C., Zanevskiy, Y., Zarochentsev, A., Zaudtke, O., Zvada,  
 P., Zbroszczyk, H., Zepeda, A., Zeter, V., Zgura, I., Zhalov, M., Zhou, D., Zhou, S., Zhu,  
 G., Zichichi, A., Zinchenko, A., Zinovjev, G., Zoccarato, Y., Zubarev, A., Zucchini, A.,  
 and Zuffa, M. (2008). The alice experiment at the cern lhc. *Journal of Instrumentation*,  
 3(08):S08002. 24

- [13] Connors, M., Nattrass, C., Reed, R., and Salur, S. (2017). Review of Jet Measurements in Heavy Ion Collisions. vi, 11, 14
- [14] Elia, D. and the ALICE Collaboration (2013). Strangeness production in alice. *Journal of Physics: Conference Series*, 455(1):012005. 18
- [15] Evans, L. and Bryant, P. (2008). Lhc machine. *Journal of Instrumentation*, 3(08):S08001. 9
- [16] Foka, P. and Janik, M. A. (2016). An overview of experimental results from ultra-relativistic heavy-ion collisions at the cern lhc: Bulk properties and dynamical evolution. *Reviews in Physics*, 1:154 – 171. 10
- [17] Gyulassy, M. (2004). The QGP discovered at RHIC. In *Structure and dynamics of elementary matter. Proceedings, NATO Advanced Study Institute, Camyuva-Kemer, Turkey, September 22-October 2, 2003*, pages 159–182. 7
- [18] Hilke, H. J. (2010). Time projection chambers. *Reports on Progress in Physics*, 73(11):116201. vii, 26, 27
- [19] Huovinen, P., Kolb, P. F., Heinz, U., Ruuskanen, P. V., and Voloshin, S. A. (2001). Radial and elliptic flow at RHIC: further predictions. *Physics Letters B*, 503:58–64. 16
- [20] Jacobs, P. and Wang, X.-N. (2005). Matter in extremis: ultrarelativistic nuclear collisions at RHIC. *Progress in Particle and Nuclear Physics*, 54:443–534. 15
- [21] Kapusta, J. I. (1979). Quantum chromodynamics at high temperature. *Nuclear Physics B*, 148(3):461 – 498. 3
- [22] Luo, X. (2016). Exploring the qcd phase structure with beam energy scan in heavy-ion collisions. *Nuclear Physics A*, 956:75 – 82. The XXV International Conference on Ultrarelativistic Nucleus-Nucleus Collisions: Quark Matter 2015. 27
- [23] Martinez, G. (2013). Advances in Quark Gluon Plasma. *ArXiv e-prints*. 6
- [24] Nattrass, C. (2009). System, energy, and flavor dependence of jets through di-hadron correlations in heavy ion collisions. v, 10, 26

- [25] Odyniec, G. (2013). The rhic beam energy scan program in star and what's next ...  
*Journal of Physics: Conference Series*, 455(1):012037. 27
- [26] Ozaki, S. and Roser, T. (2015). Relativistic heavy ion collider, its construction and  
 upgrade. *Progress of Theoretical and Experimental Physics*, 2015(3):03A102. vi, 8
- [27] Preghenella, R. (2011). Transverse momentum spectra of identified charged hadrons  
 with the ALICE detector in Pb-Pb collisions at  $\sqrt{s_{NN}} = 2.76$  TeV. *PoS, EPS-*  
*HEP2011:118*. 24
- [28] Qin, G.-Y. and Wang, X.-N. (2015). Jet quenching in high-energy heavy-ion collisions.  
*International Journal of Modern Physics E*, 24:1530014–438. 19
- [29] Satz, H. (2006). Colour deconfinement and quarkonium binding. *Journal of Physics G:*  
*Nuclear and Particle Physics*, 32(3):R25. 4, 6
- [30] Schenke, B. (2017). Origins of collectivity in small systems. *Nuclear Physics A*, 967:105  
 – 112. The 26th International Conference on Ultra-relativistic Nucleus-Nucleus Collisions:  
 Quark Matter 2017. 16
- [31] Shao, M., Barannikova, O. Yu., Dong, X., Fisyak, Y., Ruan, L., Sorensen, P., and Xu,  
 Z. (2006). Extensive particle identification with TPC and TOF at the STAR experiment.  
*Nucl. Instrum. Meth.*, A558:419–429. 26
- [32] Shuryak, E. V. (1988). The qcd vacuum and quark-gluon plasma. *Zeitschrift für Physik*  
*C Particles and Fields*, 38(1):141–145. 3
- [33] Snellings, R. (2011). Elliptic flow: a brief review. *New Journal of Physics*, 13(5):055008.  
 16
- [34] Stock, R. (2004). Ultra-relativistic nucleus-nucleus collisions. Proceedings, 17th  
 International Conference, Quark Matter 2004, Oakland, USA, January 11-17, 2004. *J.*  
*Phys.*, G30:S633–S648. 7
- [35] Strickland, M. (2014). Anisotropic hydrodynamics: Motivation and methodology.  
*Nuclear Physics A*, 926:92–101. 16

- 1472 [36] Stcker, H. (2005). Collective flow signals the quarkgluon plasma. *Nuclear Physics A*,  
1473 750(1):121 – 147. Quark-Gluon Plasma. New Discoveries at RHIC: Case for the Strongly  
1474 Interacting Quark-Gluon Plasma. Contributions from the RBRC Workshop held May 14-  
1475 15, 2004. vii, 21
- 1476 [37] Vovchenko, V., Anchishkin, D., and Csernai, L. P. (2014). Time dependence of  
1477 partition into spectators and participants in relativistic heavy-ion collisions. *Phys. Rev.*  
1478 *C*, 90:044907. vi, 12
- 1479 [38] Wilde, M. (2013). Measurement of Direct Photons in pp and Pb-Pb Collisions with  
1480 ALICE. *Nucl. Phys.*, A904-905:573c–576c. 18
- 1481 [39] Wong, C.-Y. (1994). *Introduction to high-energy heavy-ion collisions*. World scientific.  
1482 vi, 12, 17, 18, 19, 20

# Appendices